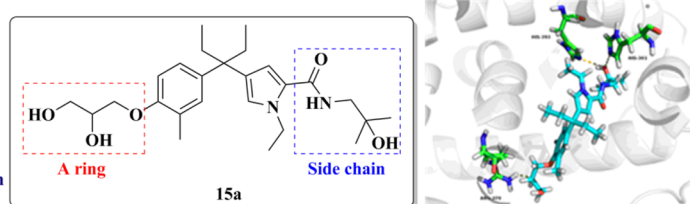


## Design, Synthesis, and Antifibrosis Activity in Liver of Nonsteroidal Vitamin D Receptor Agonists with Phenyl-pyrrolyl Pentane Skeleton

Cong Wang,<sup>†,‡,§</sup> Bin Wang,<sup>†,§</sup> Lingjing Xue,<sup>†</sup> Zisheng Kang,<sup>†</sup> Siyuan Hou,<sup>†</sup> Junjie Du,<sup>†</sup> and Can Zhang<sup>\*,†,§</sup><sup>†</sup>State Key Laboratory of Natural Medicines and Jiangsu Key Laboratory of Drug Discovery for Metabolic Diseases, Center of New Drug Discovery, China Pharmaceutical University, 24 Tong Jia Xiang, Nanjing 210009, China<sup>‡</sup>Fujian Provincial Key Laboratory of Hepatic Drug Research, Fuzhou 350001, China

## Supporting Information

Good VDR agonistic activity  
Significantly decreased the synthesis of collagen 1 *in vitro*  
Markedly prevented in the progress of liver fibrosis  
Improvements in liver function



**ABSTRACT:** Liver fibrosis is characterized by excessive deposition of extracellular matrix (ECM) components and results in impaired liver function. Vitamin D plays a critical role in the development of liver fibrosis as it inhibits transforming growth factor  $\beta 1$  (TGF $\beta 1$ )-induced excessive deposition of ECM in activated hepatic stellate cells (HSCs). Here, a series of novel nonsteroidal vitamin D receptor (VDR) agonists with phenyl-pyrrolyl pentane skeleton was designed and synthesized. Among them, seven compounds including **15a** exhibited more efficient inhibitory activity in collagen deposition and fibrotic gene expression. Histological examination results displayed that compound **15a** treatment prevented the development of hepatic fibrosis that induced by carbon tetrachloride (CCl<sub>4</sub>) injections in mice. In addition, compound **15a**, unlike the positive control calcipotriol and 1,25(OH)<sub>2</sub>D<sub>3</sub>, did not cause hypercalcemia that is toxic to nerve, heart, and many other organs. These findings provide novel insights into drug discoveries for hepatic fibrosis using nonsteroidal VDR modulators.

## INTRODUCTION

Liver fibrosis, characterized by excessive accumulation of extracellular matrix (ECM) and loss of pliability and liver function, is the result of wound-healing responses that were triggered by either chronic or acute liver injury,<sup>1–3</sup> such as alcohol abuse, chronic hepatitis virus (hepatitis B virus/hepatitis C virus) infection, and, increasingly, nonalcoholic steatohepatitis (NASH) and nonalcoholic fatty liver disease (NAFLD).<sup>4–6</sup> With continuous injury, the fibrillar collagens were progressively deposited and parenchymal nodules were surrounded by collagen bands, eventually leading to the histological signature of hepatic cirrhosis, which represents a major global health concern. At present, the only way to treat the end-stage cirrhosis is liver transplantation.<sup>7</sup> However, the condition of the potential recipients, especially the number of available donor organs, limited the applicability of this technique even in the developed world.<sup>8</sup> Moreover, the Food and Drug Administration has not yet approved antifibrotic therapies for chronic liver disease.<sup>9</sup>

Hepatic stellate cells (HSCs) are established as a major cellular source of ECM and the main driver of liver fibrogenesis. In healthy liver cells, HSCs remains quiescent, and the main function is storing vitamin A.<sup>10</sup> Once being

activated following liver injury, HSCs would enter into a  $\alpha$ -smooth muscle actin ( $\alpha$ -SMA) positive phenotypic transformation and differentiate into ECM-secreting cells. The activated HSCs produce a considerable amount of collagen I, which is the main component of ECM, resulting in the loss of liver pliability and function.<sup>11</sup>

Transforming growth factor  $\beta 1$  (TGF $\beta 1$ ) is one of the most potent pro-fibrotic modulators. In paracrine and autocrine fashion, TGF $\beta 1$  promotes HSC activation and contributes to fibrotic processes in liver.<sup>12,13</sup> Therefore, the inhibition of TGF $\beta 1$  pathway to reduce ECM production in HSCs is recognized as an effective antifibrotic strategy. While the precise mechanisms of regulating ECM synthesis via TGF $\beta 1$  pathway have yet to be elucidated, vitamin D has been established in a close relationship with TGF $\beta 1$  and liver fibrosis development. Previous studies demonstrated a beneficial effect for 1,25(OH)<sub>2</sub>D<sub>3</sub> (**1**, Figure 1), the most active form of vitamin D, to attenuate liver fibrosis.<sup>14–16</sup>

It is widely recognized that 1,25(OH)<sub>2</sub>D<sub>3</sub> plays a pivotal role in the homeostasis of calcium and phosphorus, cell

Received: July 26, 2018

Published: October 10, 2018

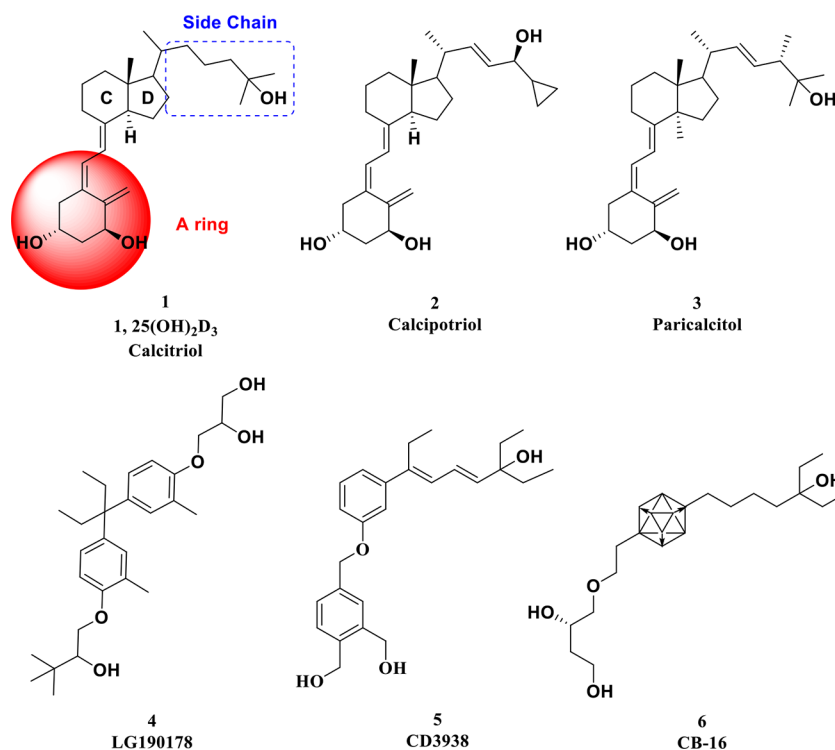


**Figure 1.** Chemical structures of representative secosteroidal and nonsecosteroidal VDR ligands.

proliferation and differentiation, as well as immunomodulation.<sup>17,18</sup> 1,25(OH)<sub>2</sub>D<sub>3</sub> exerts actions through promoting gene transcription by binding to vitamin D receptor (VDR), which belonging to the superfamily of nuclear receptor. VDR is robustly expressed in HSCs and fully functional in these cells.<sup>19</sup> In 2013, Ding et al. reported that calcipotriol, an analog of 1,25(OH)<sub>2</sub>D<sub>3</sub>, could inhibit the collagen I and  $\alpha$ -SMA expression via reducing the occupancy of SMAD3 at these sites and antagonizing a wide range of transcriptional responses on profibrotic genes that depend on TGF $\beta$ /SMAD signaling pathway.<sup>20</sup> These findings suggest that VDR is a checkpoint to modulate the liver wound-healing response and that VDR ligands may serve as a potential therapy for the treatment of liver fibrosis.

VDR ligands have already been attractive therapeutics against psoriasis, osteoporosis, and cancer.<sup>21–23</sup> At present, more than 3000 VDR modulators with secosteroid skeleton have been synthesized and biologically evaluated as drug candidates,<sup>24</sup> such as calcipotriol (2) and paricalcitol (3). Almost all of the VDR ligands with high activity have the same secosteroidal skeleton as 1–3, structurally consisting of the A-ring that borne two hydroxyl groups, a triene moiety or conjugated diene, a side chain, and the CD ring. Although many compounds exhibit efficient VDR activity in *in vitro* and *in vivo* studies, their synthetic inconvenience, structural complexity, chemical instability, and hypercalcemia limit the clinical application in the treatment of liver fibrosis. Recently, a lot of attention has been drawn to nonsecosteroidal vitamin D mimics,<sup>25–28</sup> such as bisphenol derivative (4),<sup>29</sup> tris-aromatic derivatives (5),<sup>21</sup> and carborane derivatives (6),<sup>30–33</sup> due to their less calcium mobilization and simpler structures. Previously, we have reported phenyl-pyrrolyl pentane skeleton as a novel nonsecosteroidal VDR ligand skeleton, which possessed the potential to inhibit proliferation of cancer cells without inducing hypercalcemia effect.<sup>34–36</sup> However, we

found that some compounds had no effect on cancer cells but show significant inhibitory effect on HSCs activation, indicating that VDR agonists may affect HSCs more strongly than cancer cells. Therefore, it is noteworthy to verify whether these nonsecosteroidal vitamin D ligands can act as effective as 1,25(OH)<sub>2</sub>D<sub>3</sub> or calcipotriol that with secosteroidal skeleton for preventing the progression of liver fibrosis but have smaller side effects like hypercalcemia.

To explore the relationship between structure and antifibrotic activity for these nonsecosteroidal compounds based on the phenyl-pyrrolyl pentane skeleton, 22 new compounds have been designed, synthesized, and examined with various biological assays. Seven compounds showed much better properties than positive control calcipotriol in the anticollagen I synthetic activities assay. Among them, compound 15a exhibited more potent inhibitory activity against both fibrotic gene expression and collagen deposition by Q-PCR and Western blot assays. Results of histological examination displayed that the treatment of compound 15a prevented hepatic fibrosis induced by carbon tetrachloride (CCl<sub>4</sub>) injection in mice. Moreover, compound 15a had no significant change on serum calcium that can be raised by positive control calcipotriol or 1,25(OH)<sub>2</sub>D<sub>3</sub>.

## RESULTS AND DISCUSSION

**Design of Target Compounds.** Boehm et al. reported the first nonsecosteroidal analogs of vitamin D<sub>3</sub>, LG190178 (4), and found that propane-1,2-diol of 4 are important for the binding affinity. Based on the phenyl-pyrrolyl pentane skeleton and the structure feature of 4, we designed derivatives 13 using a scaffold hopping strategy and introducing different R<sub>1</sub> substituents to identify antifibrotic VDR ligands. Then, the phenyl-pentane group on the pyrrole ring C-4 position instead of the C-5 position was designed to investigate the influence of the substitution positions of the pyrrole ring, and we obtained

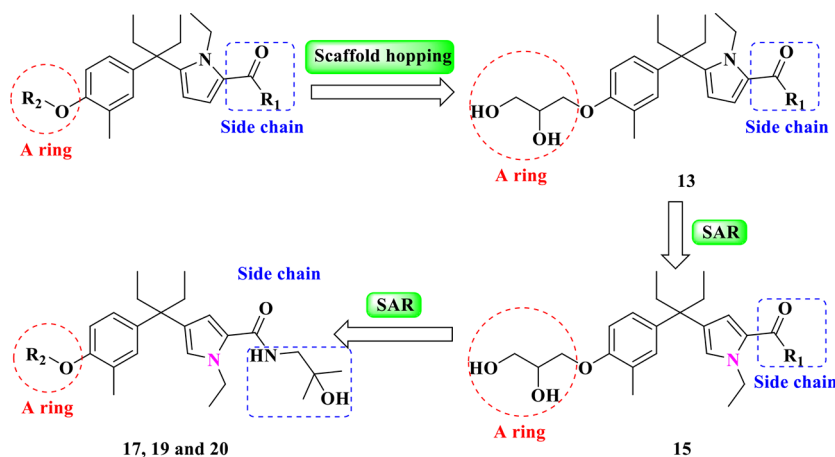
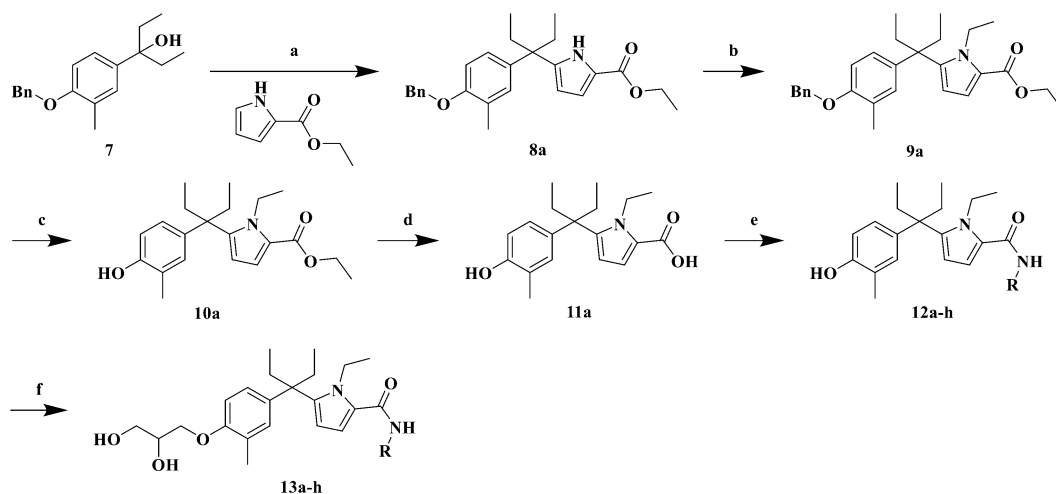


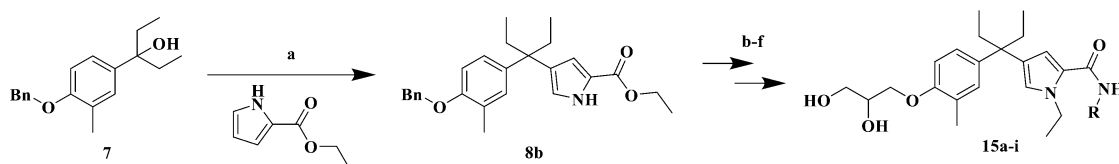
Figure 2. Design of the novel nonsecosteroidal VDR ligands.

### Scheme 1. Synthesis of Compounds 13a–h<sup>a</sup>



<sup>a</sup>Reagents and conditions: (a) ethyl 1*H*-pyrrole-2-carboxylate,  $\text{BF}_3 \cdot \text{Et}_2\text{O}$ , 0 °C, 1 h, 73%; (b)  $\text{C}_2\text{H}_5\text{I}$ , NaH, DMF, 0–25 °C, 2 h, 82.4%; (c) Pd/C,  $\text{HCOONH}_4$ ,  $\text{CH}_3\text{OH}/\text{EtOAc}$  (10:1), 25 °C, 1 h, 98%; (d) 2 mol/L KOH, EtOH, rt, 1 h, 94%; (e) EDCl, HOBT, TEA,  $\text{RNH}_2$ , DCM, rt, overnight, 35–96%; (f) glycidol, NaH, DMF, 80 °C, 5 h, 54–82%.

### Scheme 2. Synthesis of Compounds 15a–i<sup>a</sup>



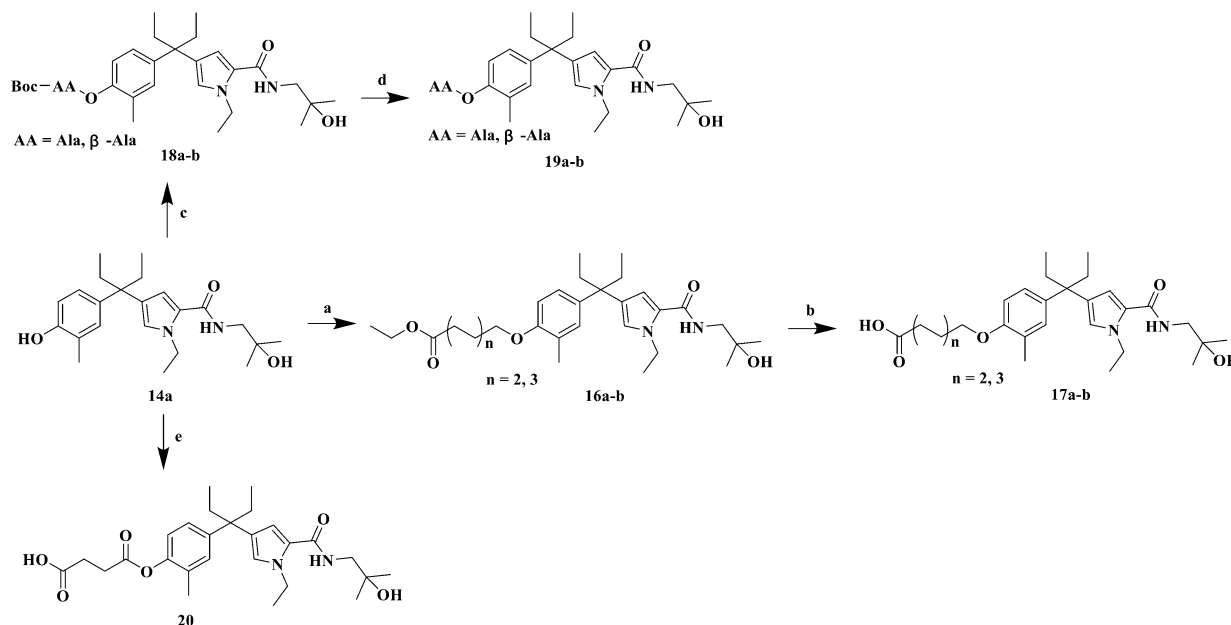
<sup>a</sup>Reagents and conditions: (a) ethyl 1*H*-pyrrole-2-carboxylate,  $\text{BF}_3 \cdot \text{Et}_2\text{O}$ , 25 °C, 1 h, 44%; (b)  $\text{C}_2\text{H}_5\text{I}$ , NaH, DMF, 0–25 °C, 2 h, 85%; (c) Pd/C,  $\text{HCOONH}_4$ ,  $\text{CH}_3\text{OH}/\text{EtOAc}$  (10:1), 25 °C, 1 h, 97%; (d) 2 mol/L KOH, EtOH, rt, 1 h, 95%; (e) EDCl, HOBT, TEA,  $\text{RNH}_2$ , DCM, rt, overnight, 32–89%; (f) glycidol, NaH, DMF, 80 °C, 5 h, 47–78%.

compounds 15. Finally, we further investigated the A ring part of target compounds and designed compounds 17, 19, and 20 by substitution of the A ring with other hydrophilic groups, such as the butanoic acid, pentanoic acid, alanine,  $\beta$ -alanine, and succinic acid (Figure 2).

**Synthetic Procedures of Target Compounds.** The synthetic pathway of target compounds 13a–h is outlined in Scheme 1. The intermediate 7 was prepared using a previously reported approach,<sup>34</sup> then it reacted with ethyl pyrrole-2-carboxylate at 0 °C in the presence of Lewis acid  $\text{BF}_3 \cdot \text{Et}_2\text{O}$  to produce intermediate 8a. After the management with iodo-

ethane in DMF, intermediate 9a was obtained. The reduction reaction of 9a gives the intermediate 10a, which was hydrolyzed by KOH to produce 11a in high yield. By reaction with the corresponding amines, 11a gave intermediates 12a–i, respectively. Finally, target compounds 13a–h were obtained by electrophilic substitution of glycidol with intermediates 12a–h in the presence of NaH.

The synthetic pathway of compounds 15a–i is outlined in Scheme 2. Intermediate 8b, the regioselectivity isomer of 8a, was obtained by reacting with ethyl pyrrole-2-carboxylate at 20 °C, instead of at 0 °C, in the presence of Lewis acid  $\text{BF}_3 \cdot \text{Et}_2\text{O}$

Scheme 3. Synthesis of Compounds 17a–b, 19a–b, and 20<sup>a</sup>

<sup>a</sup>Reagents and conditions: (a) ethyl 4-bromobutyrate or ethyl 5-bromopentylate, NaH, DMF, 80 °C, 5 h, 58–67%; (b) 2 mol/L KOH, EtOH, rt, 1 h, 95–97%; (c) Boc-AA, EDCI, DMAP, DCM, rt, overnight, 43–52%; (d) TFA, DCM, rt, 1 h, 87–92%; (e) succinic anhydride, NaH, DMF, 80 °C, 2 h, 43%.

in moderate yield. By the same method as described for the synthesis of 9a–13, target compounds 15a–i were obtained.

The synthetic pathway of compounds 17a–b, 19a–b, and 20 is outlined in Scheme 3. Intermediate 14a was subjected to nucleophilic substitution with the corresponding halo-hydrocarbon to give intermediates 16a–b, which were further treated by hydrolysis of ester groups to afford target compounds 17a–b in high yield. However, intermediates 18a–b were synthesized by treatment of intermediate 14a with corresponding amino acids. Deprotection of 18a–b using CF<sub>3</sub>COOH yielded target compounds 19a–b. Compound 20 was obtained by the same method as described in the synthesis of intermediates 16a–b.

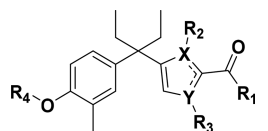
**VDR Binding Affinity.** The VDR binding affinity of synthesized compounds was tested with VDR competitor assay, and 1,25(OH)<sub>2</sub>D<sub>3</sub> was applied as the positive control. All compounds were evaluated for their binding affinity in triplicates at 100 nM. The binding affinity of compounds was exhibited by a reference value to 1,25(OH)<sub>2</sub>D<sub>3</sub>, which is assigned as 100%. Tables 1 and 2 showed the structure–activity relationships (SARs) for these compounds. First, we focused on the important pharmacophore side chain of the pyrrole ring at the C-5 position bearing a phenyl-pentane group; the results showed that compounds with the terminal hydrophobic groups in the side chain section, such as *tert*-butoxide (13a), *tert*-butyl (13b), trifluoromethyl (13e), displayed significant binding affinities. However, introducing flexible hydrophobic substitution of the *n*-pentyl group to give compound 13h resulted in decreased affinity, which suggests that flexible substitution is not preferred in the VDR ligand binding pocket (LBP). Moreover, substitutions of hydrophilic groups, such as 1-hydroxy (13d) and aminos (13f–g), dramatically decreased the binding affinities. By removing the substitution on the pyrrole group C-5 position to C-4 position, compounds 15a–i were synthesized to explore the influence of substitution position on the binding affinity. Although most

compounds displayed decreased binding affinities compared to the pyrrole group C-5 position, compound 15a bearing *tert*-butoxide group showed better activity than the corresponding compound 13a and turned out to be the most potent molecule. Subsequently, we further investigated the A ring part of target compounds by substitution of the A ring with other hydrophilic groups, such as butanoic acid (17a), pentanoic acid (17b), alanine (19a),  $\beta$ -alanine (19b), and butanedioic acid (20). As a result, no improvement of the binding affinities was detected compared with that of compound 15a. Meanwhile, carboxylic acid as the terminal hydrophilic group, such as in compounds 17a–b and 20, displayed better binding affinities than that of amine groups (19a–b).

**Transactivation.** To estimate agonistic abilities of the nonsteroidal ligands bearing phenyl-pyrrolyl pentane skeleton, a transactivation assay was performed in HEK293 cells using pGL4.27-SPP  $\times$  3-*Luci* reporter plasmid. Compounds 13a–b, 15a, and 15e with strong binding affinities were selected, and calcipotriol and 1,25(OH)<sub>2</sub>D<sub>3</sub> were used as positive controls. As shown in Figure 3, all four compounds acted as potent agonists with concentration-dependent transcriptional activity. Among them, compound 15a was the most potent compound and displayed transcriptional activity at 100 nM, while compounds 13a–b and 15e did not reach the optimal transcription level even at 1000 nM. This may be due to the interaction of heterodimer partners with VDR, such as nuclear receptor corepressor 1 and steroid receptor coactivator 1, which has an effect on the biological activity of VDR. In addition, a significantly higher increase of transcripts encoding 25-hydroxyvitamin D-24-hydroxylase (*CYP24A1*) by compounds 15a was shown (Figure S1).

**Anticollagen I Synthetic Activities *in Vitro*.** Liver fibrosis is characterized by the replacement of functional hepatic tissue with highly cross-linked collagen I-rich ECM, and TGF $\beta$ 1 is recognized as one of the most potent pro-fibrotic modulators responsible for collagen I synthesis.

Table 1. Structures of All Compounds



| Compd | X | Y | R <sub>1</sub> | R <sub>2</sub>                | R <sub>3</sub>                | R <sub>4</sub> | Compd | X | Y | R <sub>1</sub> | R <sub>2</sub> | R <sub>3</sub>                | R <sub>4</sub> |
|-------|---|---|----------------|-------------------------------|-------------------------------|----------------|-------|---|---|----------------|----------------|-------------------------------|----------------|
| 13a   | N | C |                | C <sub>2</sub> H <sub>5</sub> | H                             |                | 15d   | C | N |                | H              | C <sub>2</sub> H <sub>5</sub> |                |
| 13b   | N | C |                | C <sub>2</sub> H <sub>5</sub> | H                             |                | 15e   | C | N |                | H              | C <sub>2</sub> H <sub>5</sub> |                |
| 13c   | N | C |                | C <sub>2</sub> H <sub>5</sub> | H                             |                | 15f   | C | N |                | H              | C <sub>2</sub> H <sub>5</sub> |                |
| 13d   | N | C |                | C <sub>2</sub> H <sub>5</sub> | H                             |                | 15g   | C | N |                | H              | C <sub>2</sub> H <sub>5</sub> |                |
| 13e   | N | C |                | C <sub>2</sub> H <sub>5</sub> | H                             |                | 15h   | C | N |                | H              | C <sub>2</sub> H <sub>5</sub> |                |
| 13f   | N | C |                | C <sub>2</sub> H <sub>5</sub> | H                             |                | 15i   | C | N |                | H              | C <sub>2</sub> H <sub>5</sub> |                |
| 13g   | N | C |                | C <sub>2</sub> H <sub>5</sub> | H                             |                | 17a   | C | N |                | H              | C <sub>2</sub> H <sub>5</sub> |                |
| 13h   | N | C |                | C <sub>2</sub> H <sub>5</sub> | H                             |                | 17b   | C | N |                | H              | C <sub>2</sub> H <sub>5</sub> |                |
| 15a   | C | N |                | H                             | C <sub>2</sub> H <sub>5</sub> |                | 19a   | C | N |                | H              | C <sub>2</sub> H <sub>5</sub> |                |
| 15b   | C | N |                | H                             | C <sub>2</sub> H <sub>5</sub> |                | 19b   | C | N |                | H              | C <sub>2</sub> H <sub>5</sub> |                |
| 15c   | C | N |                | H                             | C <sub>2</sub> H <sub>5</sub> |                | 20    | C | N |                | H              | C <sub>2</sub> H <sub>5</sub> |                |

Consequently, inhibiting the production of collagen I induced by TGF $\beta$ 1 is an effective strategy against fibrotic progress. To examine the antifibrotic effects of all target compounds, a stable and unlimited source of human HSCs, LX-2 cells, was employed as a valuable cell model to study human hepatic fibrosis. Calcipotriol and 1,25(OH)<sub>2</sub>D<sub>3</sub> were applied as positive control (Table 2). Compared with calcipotriol and 1,25(OH)<sub>2</sub>D<sub>3</sub>, seven of the synthesized analogues (13a–b, 13e, 15a–b, 15e, and 17a) at the concentration of 100 nM, which was little cytotoxic to LX-2 (Table S1), demonstrated more effective inhibitory properties against collagen I synthesis, with the values at the range of 112–210%, and six compounds (13c, 13h, 17b, 19a–b, and 20) displayed an equivalent inhibitory potency. This discrepancy between binding affinity and agonistic activity could be interpreted by the interactions between the cofactors and VDR ligand complex. It is required that the AF-2 transactivation motif of

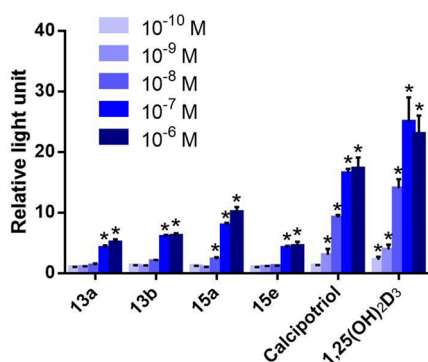
VDR interacts with cofactors such as VDR interacting proteins (DRIPs) for VDR transcriptional activation.<sup>37–39</sup> Table 2 highlights the important SAR features of inhibitory potencies. Similar to the SARs of binding affinities, 13a–b and 13e bearing terminal hydrophobic groups in the side chain section also displayed significant inhibitory activities. In addition, compound 13h, which showed decreased binding affinity compared with other compounds bearing terminal hydrophobic groups as described above, was also only moderately active. Replacement of hydrophobic groups with hydrophilic groups, such as 1-hydroxy (13d) and aminos (13f–g), dramatically weakened the inhibitory activities. On this point, it could be proved that the inhibitory activities of synthesized compounds are positively correlative with VDR binding affinities. Varying the position of the substitution from the pyrrole group on the C-5 position to the C-4 had dramatic effects on inhibitory activities. As likely as the binding affinities,



Table 2. Affinities of VDR Binding and Activities of Anticollagen I Synthetic at 100 nM

| compd | relative VDR binding ability (%) <sup>a</sup> | anticollagen I at 100 nM (%) <sup>b</sup> | compd | relative VDR binding ability (%) <sup>a</sup> | anticollagen I at 100 nM (%) <sup>b</sup> |
|-------|---|---|-------|---|---|
| 13a   | 43 ± 3.2                                      | 150 ± 13.6*                               | 15e   | 39 ± 4.8                                      | 133 ± 14.5*                               |
| 13b   | 45 ± 5.3                                      | 159 ± 9.3*                                | 15f   |   |   |
| 13c   | 27 ± 4.1                                      | 71 ± 7.2                                  | 15g   |   |   |
| 13d   |   |   | 15h   | 16 ± 1.3                                      | 51 ± 5.3                                  |
| 13e   | 37 ± 2.5                                      | 135 ± 15.9*                               | 15i   |   |   |
| 13f   |   |   | 17a   | 32 ± 3.9                                      | 112 ± 7.8                                 |
| 13g   |   |   | 17b   | 30 ± 3.2                                      | 90 ± 9.2                                  |
| 13h   | 21 ± 3.5                                      | 70 ± 7.9                                  | 19a   | 20 ± 2.9                                      | 73 ± 4.8                                  |
| 15a   | 62 ± 4.5                                      | 210 ± 20.1*                               | 19b   | 22 ± 4.8                                      | 66 ± 5.2                                  |
| 15b   | 31 ± 2.3                                      | 119 ± 7.3*                                | 20    | 30 ± 3.1                                      | 80 ± 6.1                                  |
| 15c   |   |   | 2     | 93 ± 8.5                                      | 95 ± 9.2                                  |
| 15d   |   |   | 1     | 100   | 100                                       |

<sup>a</sup>The values represent the mean ± SD of three independent experiments. 1,25(OH)<sub>2</sub>D<sub>3</sub> (1) is assigned as 100%. 1,25(OH)<sub>2</sub>D<sub>3</sub> (1) and calcipotriol (2) are the positive controls. <sup>b</sup>The values represent the mean ± SD of three independent experiments. 1,25(OH)<sub>2</sub>D<sub>3</sub> (1) is assigned as 100%. 1,25(OH)<sub>2</sub>D<sub>3</sub> (1) and calcipotriol (2) are the positive controls. \*P < 0.05 vs 1,25(OH)<sub>2</sub>D<sub>3</sub> (1).



**Figure 3.** Transcriptional activities of the compounds were examined. HEK293 cells were cotransfected with TK-SPP × 3-Luci reporter plasmid, pCMX-Renilla, pENTER-CMV-hRXR $\alpha$ , and pCMX-VDR. Eight hours after transfection, test compounds, calcipotriol, and 1,25(OH)<sub>2</sub>D<sub>3</sub> were added. Twenty-four hours later, luciferase activity assay was performed using the Dual-Luciferase Assay System. Renilla luciferase activity was given as the reference to normalize the firefly luciferase activity. All the experiments were performed three times. \*P < 0.05 vs DMSO.

compound 15a showed better activity than the corresponding compound 13a and turned out to be the most potent molecule. In addition, all compounds varying propane-1,2-diol to other hydrophilic groups displayed moderate inhibitor activities against collagen I synthesis and had no better results than 15a. Meanwhile, carboxylic acid as the terminal hydrophilic group, such as in compounds 17a–b and 20, displayed better inhibitory activities than that of amine groups (19a–b).

**Effects on the Expression of Collagen I and  $\alpha$ -SMA in LX-2 Cells.** The antifibrotic activities of selected compounds 13a, 13b, 15a, and 15e, which displayed optimal property on binding affinities and anticollagen I synthetic activities, were analyzed using Western blot and Q-PCR assays. The increased expression of collagen I and  $\alpha$ -SMA is shown by the markers of activated HSCs.<sup>3</sup> As described above, liver fibrosis, regardless of its cause, is featured by progressive accumulation of ECM proteins, and the main component is collagen I. Moreover, the  $\alpha$ -SMA-positive myofibroblasts are considered as the key promoters in the progression of liver fibrosis. Collagen I alpha 1 (COL1A1) is the direct target of VDR;<sup>20</sup> in addition,  $\alpha$ -SMA and collagen I are both upregulated by TGF $\beta$ 1 in HSCs. Therefore, the expression of  $\alpha$ -SMA and collagen I were

selected to determine the antifibrotic activities of selected compounds. As shown in Figure 4C,D, the activity of these molecules was significantly affected by the pyrrole group substitution position: compounds 15a and 15e (C-4 substitution) at the concentration of 100 nM significantly reduced  $\alpha$ -SMA and collagen I protein levels in TGF $\beta$ 1-treated LX-2 cells, while compounds 13a and 13b (C-4 substitution) exhibited no significant influence on ACTA2 expression. Compared with the hydroxyl group of analog 15a, 15e showed less activity, which suggests that a hydroxyl group in the side chain terminal is essential. Q-PCR results (Figure 4A,B) showed that compound 15a significantly down-regulated COL1A1 and ACTA2 mRNA expression. Moreover, compared with positive control calcipotriol and 1,25(OH)<sub>2</sub>D<sub>3</sub>, compound 15a showed more effective inhibitory potency against COL1A1 mRNA expression. The results impel us continuously to test the antifibrotic effect of these compounds.

**Compound 15a Inhibited Activation of LX-2 Cells through VDR.** VDR is recognized as the potential therapy target for liver fibrosis, and the above-mentioned results suggested the compounds may be VDR agonists. To confirm that compound 15a repressed fibrotic gene expression via VDR, RNA interference (RNAi) was used in LX-2 cells. Loss of VDR-abolished 15a-mediated repression of collagen I and  $\alpha$ -SMA expression was shown in Figure 5. These data demonstrated that compound 15a exerts its repressing effect on HSCs activation through interaction with VDR.

**Effects on Suppressing the Expression of  $\alpha$ -SMA in CCl<sub>4</sub>-Induced Hepatic Fibrosis Mice.** Based on *in vitro* results, compound 15a was selected for further studies *in vivo*. To explore whether compound 15a could repress the expression of fibrotic gene and inhibit hepatic fibrogenesis *in vivo*, CCl<sub>4</sub> was used to induce liver fibrosis by intraperitoneal (IP) injection in C57BL/6J mice. The antifibrotic property of compound 15a was determined by histological examination. As shown in Figure 6, consistent with the above studies *in vitro*, oral administration of compound 15a to CCl<sub>4</sub>-treated mice reduced  $\alpha$ -SMA levels in the liver tissues according to Q-PCR and IHC staining. In addition, compound 15a also increased the mRNA levels of Cyp24a1, suggesting 15a inhibits fibrotic progress through agitating VDR (Figure S2).

**Effects on Suppressing the Expression of Collagen in CCl<sub>4</sub>-Induced Hepatic Fibrosis mice.** In addition, we measured collagen content to further examine the antifibrotic

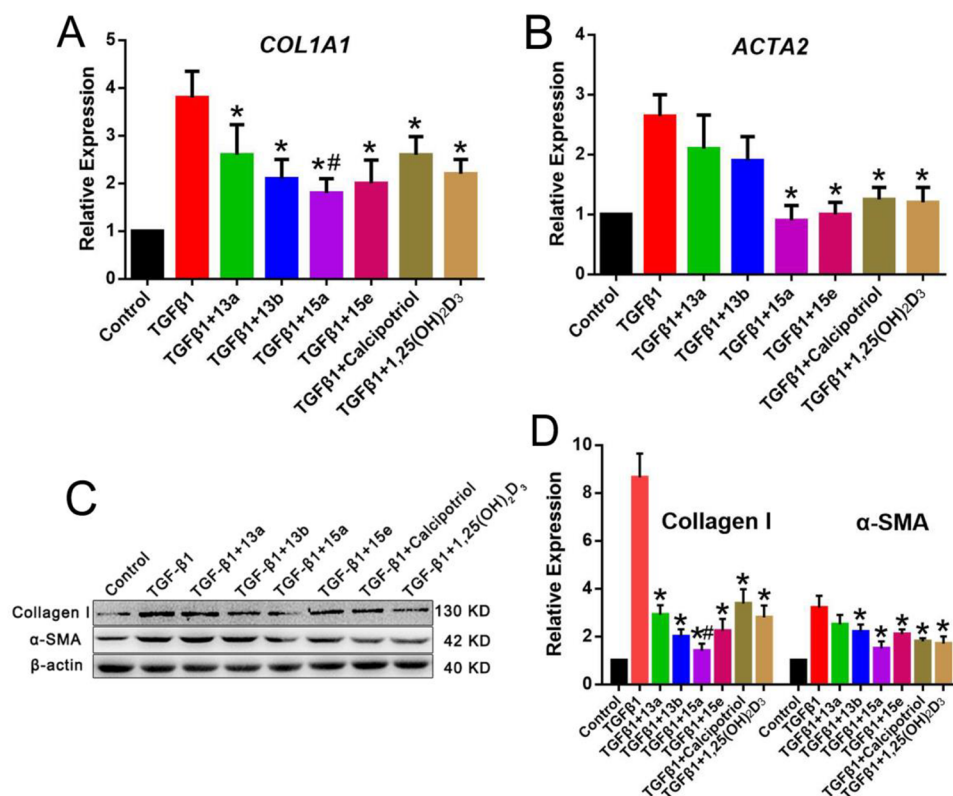


**Figure 4.** Effects of compounds on activation of LX-2 cells. LX-2 cells were cultured with compounds, calcipotriol, or 1,25(OH)<sub>2</sub>D<sub>3</sub> for 24 h at 100 nM. (A,B) Expression levels of ACTA2 and COL1A1 were measured by Q-PCR. (C,D) Expression of α-SMA and collagen I on LX-2 cells was determined by Western blot. The representative gel electrophoresis bands are shown (C), and expression levels of proteins were normalized to the expression of β-actin (D). Densitometry data are shown as mean ± SD; \**P* < 0.05 vs TGFβ1, #*P* < 0.05 vs TGFβ1 + calcipotriol.

effect of compound **15a**. Histopathologically, compound **15a** treatment resulted in the inhibition of collagen accumulation in CCl<sub>4</sub> mice liver based on H&E and Masson's trichrome staining (Figure 7A). The amounts of hepatic hydroxyproline in liver tissue were estimated, which was a major component of the collagen. As shown in Figure 7B, treatment of compound **15a** had a significant reduction in hydroxyproline content, with slightly stronger potency than positive control calcipotriol and 1,25(OH)<sub>2</sub>D<sub>3</sub>. Moreover, mRNA levels of *Coll1a1* were elevated in the liver fibrosis models, and the results showed that the expression of *Coll1a1* was also reduced by compound **15a** treatment (Figure 7C). These results suggest that compound **15a** treatment prevents CCl<sub>4</sub>-induced liver injury and hepatic fibrosis.

**Effects on Liver Function and Serum Calcium of Fibrotic Models.** Serum alanine transaminase (ALT), aspartate transaminase (AST), and total bile acid (TBA) levels are commonly measured clinically as biomarkers for liver health.<sup>40</sup> Significantly elevated levels of AST, ALT, and TBA often suggest the existence of liver damage. As shown in Figure 8A–C, the levels of AST, ALT, and TBA were significantly decreased in compound **15a**-treated mice as compared with control animals. Moreover, compound **15a** displayed better results than positive control calcipotriol and 1,25(OH)<sub>2</sub>D<sub>3</sub>, which are very promising for the reduction of liver damage. To determine the effect of novel designed nonsteroidal analogs on inducing hypercalcemic, calcium concentration was measured by calcemic activity assay *in vivo*. Ma et al. reported that nonsteroidal VDR modulators showed poor activity in intestinal cells.<sup>41</sup> Moreover, the nonsteroidal

compound has the ability to activate VDR and is weak in binding to vitamin D-binding proteins, so that it does not accumulate excessively in the intestine, resulting in no excessive calcium absorption.<sup>29</sup> In our study, compound **15a** displayed small impact on the expression of intestinal *Trpv6*, which is a VDR target gene involved in calcium metabolism (Figure S3). As shown in Figure 8D, compared with calcipotriol and 1,25(OH)<sub>2</sub>D<sub>3</sub>, there was no significant effect on serum calcium when treated with compound **15a** in mice, which suggests that nonsteroidal analog **15a** results in a high dissociation of antifibrotic potency from calcemic effects.

**In Vivo Pharmacokinetics Study.** Pharmacokinetic studies of compound **15a** and 1,25(OH)<sub>2</sub>D<sub>3</sub> were performed in rats. The results were shown in Table S3. Oral bioavailability of compound **15a** was 29.32% and *t*<sub>1/2</sub> value was 6.57 h after oral administration. Compound **15a** displayed similar bioavailability compared with 1,25(OH)<sub>2</sub>D<sub>3</sub>, whose bioavailability was 30.83% after oral administration. However, the *t*<sub>1/2</sub> value of **15a** was a little smaller compared with 1,25(OH)<sub>2</sub>D<sub>3</sub>, whose *t*<sub>1/2</sub> value was 7.55 h after oral administration. This maybe because nonsteroidal VDR agonist did not combined with vitamin D binding protein,<sup>29</sup> so the metabolism of **15a** is slightly faster. Still, the results suggested that **15a** could possess therapeutic potentials for treatment of liver fibrosis.

**Docking Analysis.** In this study, we have performed VDR binding and transactivation assays, as well as knocking down VDR gene to prove that compound **15a** represses fibrotic gene expression via VDR. To clarify the detailed interactions of VDR and the most promising compound **15a**, molecular docking study was made on the basis of the complexation of

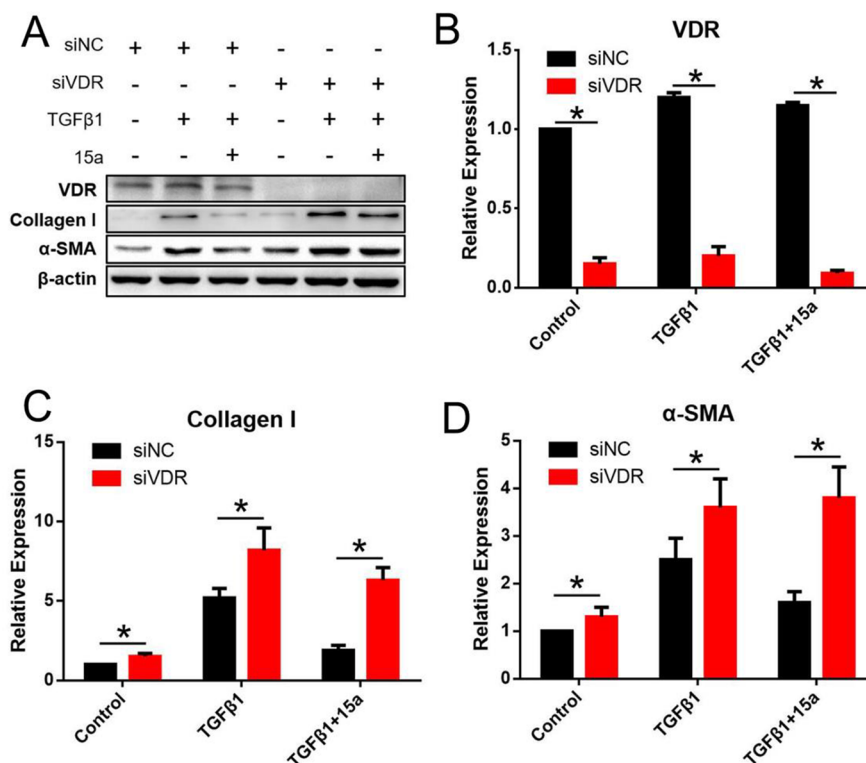


**Figure 5.** Compound 15a inhibited activation of LX-2 cells via VDR. (A) VDR-specific (siVDR) or negative control (siNC) siRNA-transfected LX-2 cells were treated with 15a (100 nM), TGFβ1 (1 ng/mL) or TGFβ1 plus 15a for 24 h. The expression of VDR, α-SMA, and collagen I on LX-2 cells was tested by Western blot. The representative gel electrophoresis bands are shown. (B–D) Expression levels of VDR, collagen I, and α-SMA were normalized to the expression of β-actin. The quantified densitometry data are shown as mean ± SD; \**P* < 0.05.

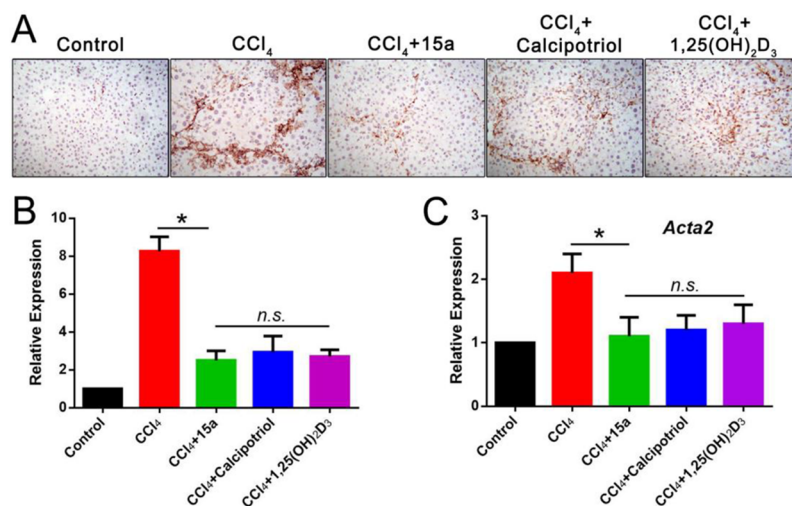


**Figure 6.** Compound 15a suppressed the expression of α-SMA in CCl<sub>4</sub>-induced hepatic fibrosis lesions and protected the liver from impairment. Mice (*n* = 5 in each group) received either DMSO or CCl<sub>4</sub> (0.5 mL/kg body weight) intraperitoneally for 3 weeks before intragastric administration of 15a, calcipotriol, 1,25(OH)<sub>2</sub>D<sub>3</sub> (20 μg/kg body weight), or DMSO. (A) α-SMA expression in the injured liver was tested by immunohistochemistry (×200). (B) Expression levels of α-SMA were quantified using Image-Pro Plus 6.0. Data are shown as mean ± SD; \**P* < 0.05 vs CCl<sub>4</sub>. (C) Expression of *Acta2* in the injured liver was examined by Q-PCR (mean ± SD; \**P* < 0.05).

the crystallographic structure of LG190178 and VDR (PDB code: 2ZFX). Using software Discovery Studio 3.0, compound 15a was manually docked into the crystal structure of VDR. Figure 9A showed the conformation superposition of compound 15a and the natural ligand 1,25(OH)<sub>2</sub>D<sub>3</sub>. Figure 9B showed the conformation superposition of compound 15a and YR301. The results demonstrated that the A ring part and side chain of compound 15a exhibited similar conformations

to those detected in the presence of YR301 and 1,25(OH)<sub>2</sub>D<sub>3</sub>. As shown in Figure 9C, the hydroxyl group of compound 15a in the side chain could form the hydrogen-bonding interactions with His 301 and His 393, which are the same for 1,25(OH)<sub>2</sub>D<sub>3</sub> bound to the hVDR LBD complex. However, the A ring part of 1,25(OH)<sub>2</sub>D<sub>3</sub> was bound with Ser 233, Arg 270, Tyr 139, and Ser 274, while compound 15a only forms a hydrogen-bonding interaction with Arg 270 by 2-



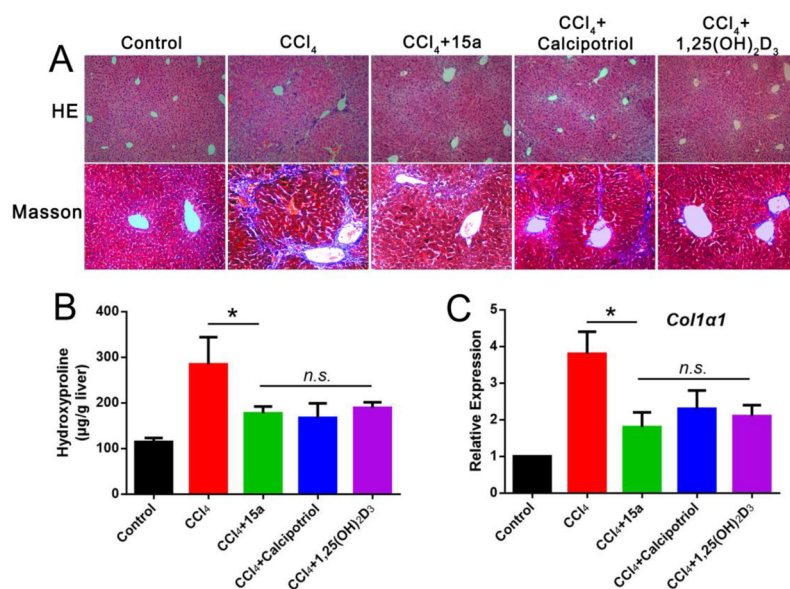


**Figure 7.** Compound 15a inhibited the CCl<sub>4</sub>-induced hepatic lesions and collagen deposition. Mice ( $n = 5$  in each group) received either DMSO or CCl<sub>4</sub> (0.5 mL/kg body weight) intraperitoneally for 3 weeks before intragastric administration of 15a, calcipotriol, 1,25(OH)<sub>2</sub>D<sub>3</sub> (20 μg/kg body weight), or DMSO. (A,B) CCl<sub>4</sub>-induced hepatic fibrosis lesions were examined by H&E staining (×100), the collagen deposition was determined by Masson's trichrome staining (×200) and hydroxyl proline measurement (mean ± SD; \* $P < 0.05$  vs CCl<sub>4</sub>). (C) Expression of *Col1a1* in the injured liver was examined by Q-PCR (mean ± SD; \* $P < 0.05$ ).

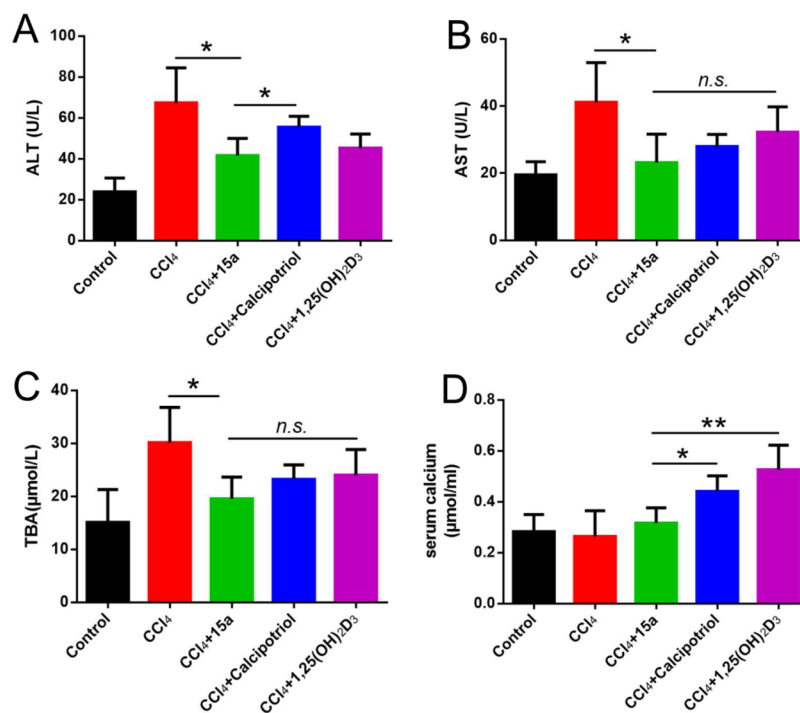


**Figure 8.** Compound 15a protected the liver from impairment. Mice ( $n = 5$  in each group) received either DMSO or CCl<sub>4</sub> (0.5 mL/kg body weight) intraperitoneally for 3 weeks before intragastric administration of 15a, calcipotriol, 1,25(OH)<sub>2</sub>D<sub>3</sub> (20 μg/kg body weight), or DMSO. (A–C) Serum levels of ALT, AST, and TBA were determined. (D) Serum calcium concentration was determined by calcium assay kit (mean ± SD; \* $P < 0.05$ , \*\* $P < 0.01$ ).

OH. This may affect the interactions of compound 15a to VDR and result in reducing binding affinity.

## CONCLUSION

In conclusion, the design, synthesis, and biological assessment of nonsteroidal derivatives with phenyl-pyrrolyl pentane skeleton have been described in this Article. The selected

compounds act as VDR agonists for effectively preventing the progression of liver fibrosis. The analysis of SARs directed the synthesis of derivative 15a, which may be a strong inhibitor for collagen I synthesis. Further exploration demonstrated that compound 15a had higher inhibitory activity on fibrotic gene expression and collagen deposition. Histological examination results displayed that compound 15a treatment prevented

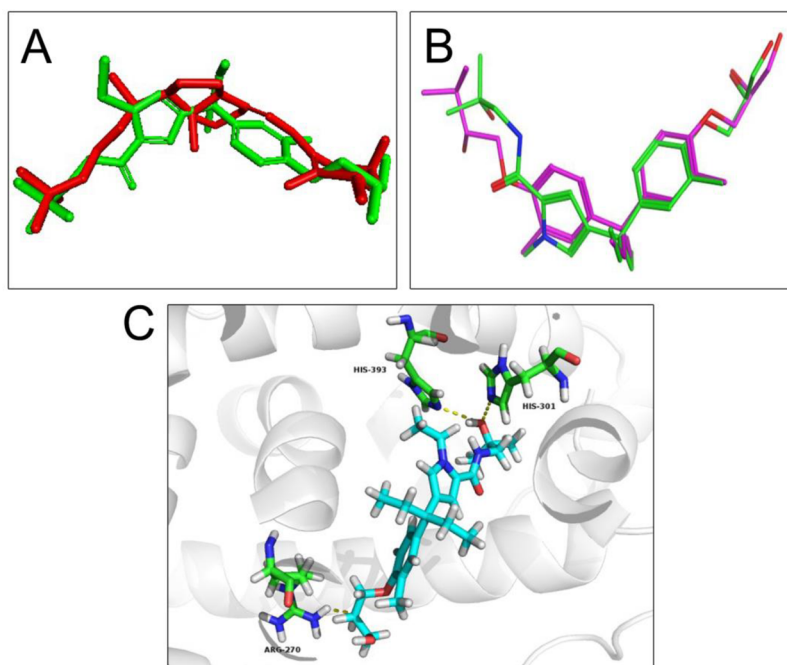


**Figure 9.** (A) Superposition of compound **15a** and  $1,25(\text{OH})_2\text{D}_3$ . Compound **15a** is depicted in green, and  $1,25(\text{OH})_2\text{D}_3$  is depicted in red. (B) Superposition of compounds **15a** and YR301. Compound **15a** is depicted in green, and YR301 is in pink. (C) Docking structure of the complex **15a**–VDR. The ligands are exhibited in stick representation where carbon is depicted in cyan and oxygen atoms in red. The hydrogen bonds that formed between ligands and VDR are exhibited as yellow dashed lines.

hepatic fibrosis induced by  $\text{CCl}_4$  injections in mice. More importantly, compound **15a** can display better results for the reduction of liver damage without significant change on serum calcium, which can be induced by positive control calcipotriol and  $1,25(\text{OH})_2\text{D}_3$ . This work supports that using non-secosteroidal VDR modulators may be applied for the treatment of hepatic fibrosis because, presently, there are still no effective therapeutic strategies.

## EXPERIMENTAL SECTION

**Chemistry. General Information.** Commercially available reagents and solvents were used without further purification. Column chromatography was carried out on Merck silica gel 60 (200–300 mesh).  $^1\text{H}$  and  $^{13}\text{C}$  NMR spectra were recorded with 300 MHz spectrometers in the indicated solvents (TMS as internal standard). Chemical shifts were reported in parts per million (ppm,  $\delta$ ) downfield from tetramethylsilane. Proton coupling patterns are described as singlet (s), doublet (d), triplet (t), quartet (q), double doublet (dd), multiplet (m), and broad (br). Purity of all tested compounds was  $\geq 95\%$ , as estimated by HPLC analysis. The major peak of the compounds analyzed by HPLC accounted for  $\geq 95\%$  of the combined total peak area when monitored by a UV detector at 254 nm. Low-resolution mass spectra (LR-MS) and high-resolution mass spectra (HR-MS) were measured on Agilent QTOF 6520.

**General Procedures. Ethyl-5-(3-(4-benzyloxy-3-methylphenyl)pentan-3-yl)-1H-pyrrole-2-carboxylate (**8a**).**  $\text{BF}_3 \cdot \text{Et}_2\text{O}$  (13 mL, 105 mmol) was added dropwise to a solution of intermediate **7** (13 g, 46 mmol) and ethyl-1H-pyrrole-2-carboxylate (7.1 g, 51 mmol) in dichloromethane (20 mL) at  $0^\circ\text{C}$ . The mixture was stirred for 1 h at  $25^\circ\text{C}$ . Then to the solution was added  $\text{H}_2\text{O}$ , and the organic phase was separated. The organic phases were washed with brine, dried over anhydrous  $\text{Na}_2\text{SO}_4$ , and evaporated. The residue was purified by column chromatography with petroleum ether/ethyl acetate (20/1, v/v) to give compound **8a** as yellow solid (13.5 g, 73% yield).

**Ethyl-4-(3-(4-(benzyloxy)-3-methylphenyl)pentan-3-yl)-1H-pyrrole-2-carboxylate (**8b**).** By the same manner as described for the preparation of **8a**, the intermediate **8b** was prepared from the

intermediate **4** and purified by silica gel chromatography with petroleum ether/ethyl acetate (12/1, v/v). Yield: 44%.

**Ethyl-5-(3-(4-(benzyloxy)-3-methylphenyl)pentan-3-yl)-1-ethyl-1H-pyrrole-2-carboxylate (**9a**).** To a solution of compound **8a** (4.05 g, 10 mmol) in DMF (5 mL), NaH (288 mg, 12 mmol) was added portion-wise at  $0^\circ\text{C}$ . After stirring for 0.5 h, ethyl iodide (1.25 g, 8 mmol) was added. The reaction mixture was stirred at  $25^\circ\text{C}$  for 2 h, and then  $\text{H}_2\text{O}$  (20 mL) was added dropwise followed by ethyl acetate (10 mL). The organic phase was separated, and the aqueous phase was extracted with ethyl acetate. The combined organic phases were washed with  $\text{H}_2\text{O}$  and brine and then dried over anhydrous  $\text{Na}_2\text{SO}_4$  and evaporated. The residue was purified by column chromatography with petroleum ether/ethyl acetate (20/1, v/v) to give compound **9a** as yellow oil (3.57 g, 82.4% yield).

**Ethyl-4-(3-(4-(benzyloxy)-3-methylphenyl)pentan-3-yl)-1-ethyl-1H-pyrrole-2-carboxylate (**9b**).** By the same manner as described for the preparation of **9a**, the intermediate **9b** was prepared from the intermediate **8b** and purified by silica gel chromatography with petroleum ether/ethyl acetate (20/1, v/v). Yield: 85%.

**Ethyl-1-ethyl-5-(3-(4-hydroxy-3-methylphenyl)pentan-3-yl)-1H-pyrrole-2-carboxylate (**10a**).** To a solution of intermediate **9a** (2.0 g, 4.6 mmol) in methanol (20 mL), Pd/C (0.2 g) and ammonium formate (2.9 g, 46 mmol) were added. The reaction mixture was stirred at  $25^\circ\text{C}$  overnight. The precipitate was filtered off, and  $\text{H}_2\text{O}$  (100 mL) and ethyl acetate (50 mL) were added to the solution. The organic phase was separated, and the aqueous phase was extracted with ethyl acetate. The combined organic phases were washed with brine, dried over anhydrous  $\text{Na}_2\text{SO}_4$ , and evaporated to give compound **10a** as white solid (1.55 g, 98% yield).

**Ethyl-1-ethyl-4-(3-(4-hydroxy-3-methylphenyl)pentan-3-yl)-1H-pyrrole-2-carboxylate (**10b**).** By the same manner as described for the preparation of **10a**, the intermediate **10b** was prepared from the intermediate **9b**. Yield: 97%.

**1-Ethyl-5-(3-(4-hydroxy-3-methylphenyl)pentan-3-yl)-1H-pyrrole-2-carboxylic acid (**11a**).** The intermediate **10a** (351 mg, 1 mmol) was dissolved in ethanol (6 mL) and treated with KOH (168 mg, 3 mmol) in  $\text{H}_2\text{O}$ , and the reaction mixture was stirred at  $80^\circ\text{C}$  for 5 h. The solution was diluted with  $\text{H}_2\text{O}$  (20 mL), and the pH value was adjusted to about 3–4 using 1 M HCl. Then, it was

extracted with ethyl acetate. The aqueous phase was extracted with ethyl acetate. The combined organic phases were washed with brine and then dried over anhydrous  $\text{Na}_2\text{SO}_4$  and evaporated. The residue was purified by column chromatography with petroleum ether/ethyl acetate (10/1, v/v) to give the intermediate **11a** as yellow oil (307 mg, 94%).

**1-Ethyl-4-(3-(4-hydroxy-3-methylphenyl)pentan-3-yl)-1H-pyrrole-2-carboxylic acid (11b)**. By the same manner as described for the preparation of **11a**, the intermediate **11b** was prepared from the intermediate **10b**. Yield: 95%.

**1-Ethyl-N-(2-hydroxy-2-methylpropyl)-5-(3-(4-hydroxy-3-methylphenyl)pentan-3-yl)-1H-pyrrole-2-carboxamide (12a)**. To a solution of compound **11a** (250 mg, 0.61 mmol) in  $\text{CH}_2\text{Cl}_2$  (10 mL) was added  $\text{Et}_3\text{N}$  (255  $\mu\text{L}$ , 1.83 mmol), followed by 1-amino-2-methylpropan-2-ol (153 mg, 1.22 mmol), EDCI (175 mg, 0.92 mmol), and HOBt (124 mg, 0.92 mmol). The reaction mixture was stirred at 25 °C overnight and then poured into  $\text{H}_2\text{O}$ . The solution was extracted with  $\text{CH}_2\text{Cl}_2$ , and the aqueous phase was extracted with  $\text{CH}_2\text{Cl}_2$ . The combined organic phases were washed with  $\text{H}_2\text{O}$  and brine, then dried over anhydrous  $\text{Na}_2\text{SO}_4$  and evaporated. The residue was purified by column chromatography with petroleum ether/ethyl acetate (4/1, v/v) to give compound **12a** as white solid (233 mg, 82% yield).

**1-Ethyl-5-(3-(4-hydroxy-3-methylphenyl)pentan-3-yl)-N-neopentyl-1H-pyrrole-2-carboxamide (12b)**. By the same manner as described for the preparation of **12a**, the intermediate **12b** was prepared from the intermediate **11a**. Yield: 78%.

**N-(Cyclopropylmethyl)-1-ethyl-5-(3-(4-hydroxy-3-methylphenyl)pentan-3-yl)-1H-pyrrole-2-carboxamide (12c)**. By the same manner as described for the preparation of **12a**, the intermediate **12c** was prepared from the intermediate **11a**. Yield: 57%.

**Methyl(1-ethyl-5-(3-(4-hydroxy-3-methylphenyl)pentan-3-yl)-1H-pyrrole-2-carbonyl)glycinate (12d)**. By the same manner as described for the preparation of **12a**, the intermediate **12d** was prepared from the intermediate **11a**. Yield: 57%.

**1-Ethyl-5-(3-(4-hydroxy-3-methylphenyl)pentan-3-yl)-N-(2-hydroxyethyl)-1H-pyrrole-2-carboxamide (12d-OH)**. To a solution of **12d** (114 mg, 0.23 mmol) in ethyl acetate (10 mL),  $\text{LiAlH}_4$  (13 mg, 0.35 mmol) was added portion-wise at 0 °C. The reaction mixture was stirred at 25 °C for 1 h, and then  $\text{H}_2\text{O}$  (10 mL) was added. The solution was extracted with ethyl acetate, and aqueous phase was extracted with ethyl acetate. The combined organic phases were washed with brine and then dried over anhydrous  $\text{Na}_2\text{SO}_4$  and evaporated. The residue was purified by column chromatography with petroleum ether/ethyl acetate (1/1, v/v) to give compound **12d-OH** as white solid (100 mg, 96% yield).

**1-Ethyl-5-(3-(4-hydroxy-3-methylphenyl)pentan-3-yl)-N-(2,2,2-trifluoroethyl)-1H-pyrrole-2-carboxamide (12e)**. By the same manner as described for the preparation of **12a**, the intermediate **12e** was prepared from the intermediate **11a**. Yield: 45%.

**N-(3-(Dimethylamino)propyl)-1-ethyl-5-(3-(4-hydroxy-3-methylphenyl)pentan-3-yl)-1H-pyrrole-2-carboxamide (12f)**. By the same manner as described for the preparation of **12a**, the intermediate **12f** was prepared from the intermediate **11a**. Yield: 68%.

**N-(2-(Dimethylamino)ethyl)-1-ethyl-5-(3-(4-hydroxy-3-methylphenyl)pentan-3-yl)-1H-pyrrole-2-carboxamide (12g)**. By the same manner as described for the preparation of **12a**, the intermediate **12g** was prepared from the intermediate **11a**. Yield: 62%.

**1-Ethyl-5-(3-(4-hydroxy-3-methylphenyl)pentan-3-yl)-N-pentyl-1H-pyrrole-2-carboxamide (12h)**. By the same manner as described for the preparation of **12a**, the intermediate **12g** was prepared from the intermediate **11a**. Yield: 87%.

**5-(3-(4-(2,3-Dihydroxypropoxy)-3-methylphenyl)pentan-3-yl)-1-ethyl-N-(2-hydroxy-2-methylpropyl)-1H-pyrrole-2-carboxamide (13a)**. To a solution of intermediate **12a** (386 mg, 1 mmol) in DMF,  $\text{NaH}$  (80 mg, 2 mmol) was added portion-wise at 0 °C. The reaction mixture was stirred at 0 °C for 1 h, and then glycidol (0.1 mL, 1.5 mmol) was added. The reaction mixture was moved to 80 °C for 5 h and then  $\text{H}_2\text{O}$  (10 mL) was added. The solution was extracted with ethyl acetate, and aqueous phase was extracted with ethyl acetate. The combined organic phases were washed with brine and then dried over

anhydrous  $\text{Na}_2\text{SO}_4$  and evaporated. The residue was purified by column chromatography ( $\text{CH}_2\text{Cl}_2/\text{CH}_3\text{OH} = 50/1$ ) to give compound **13a** as white solid (245 mg, 53% yield).

**5-(3-(4-(2,3-Dihydroxypropoxy)-3-methylphenyl)pentan-3-yl)-1-ethyl-N-neopentyl-1H-pyrrole-2-carboxamide (13b)**. By the same manner as described for the preparation of **13a**, compound **13b** was prepared from the intermediate **12b**. Yield: 87%.

**N-(Cyclopropylmethyl)-5-(3-(4-(2,3-dihydroxypropoxy)-3-methylphenyl)pentan-3-yl)-1-ethyl-1H-pyrrole-2-carboxamide (13c)**. By the same manner as described for the preparation of **13a**, compound **13c** was prepared from the intermediate **12c**. Yield: 44%.

**5-(3-(4-(2,3-Dihydroxypropoxy)-3-methylphenyl)pentan-3-yl)-1-ethyl-N-(2-hydroxyethyl)-1H-pyrrole-2-carboxamide (13d)**. By the same manner as described for the preparation of **13a**, compound **13d** was prepared from the intermediate **12d-OH**. Yield: 35%.

**5-(3-(4-(2,3-Dihydroxypropoxy)-3-methylphenyl)pentan-3-yl)-1-ethyl-N-(2,2,2-trifluoroethyl)-1H-pyrrole-2-carboxamide (13e)**. By the same manner as described for the preparation of **13a**, compound **13e** was prepared from the intermediate **12e**. Yield: 68%.

**5-(3-(4-(2,3-Dihydroxypropoxy)-3-methylphenyl)pentan-3-yl)-N-(3-(dimethylamino)propyl)-1-ethyl-1H-pyrrole-2-carboxamide (13f)**. By the same manner as described for the preparation of **13a**, compound **13f** was prepared from the intermediate **12f**. Yield: 78%.

**N-(3-(Diethylamino)propyl)-5-(3-(4-(2,3-dihydroxypropoxy)-3-methylphenyl)pentan-3-yl)-1-ethyl-1H-pyrrole-2-carboxamide (13g)**. By the same manner as described for the preparation of **13a**, compound **13g** was prepared from the intermediate **12g**. Yield: 64%.

**5-(3-(4-(2,3-Dihydroxypropoxy)-3-methylphenyl)pentan-3-yl)-1-ethyl-N-pentyl-1H-pyrrole-2-carboxamide (13h)**. By the same manner as described for the preparation of **13a**, compound **13h** was prepared from the intermediate **12h**. Yield: 96%.

**4-(3-(4-(2,3-Dihydroxypropoxy)-3-methylphenyl)pentan-3-yl)-1-ethyl-N-(2-hydroxy-2-methylpropyl)-1H-pyrrole-2-carboxamide (14a)**. By the same manner as described for the preparation of **12a**, the intermediate **14a** was prepared from the intermediate **11b**. Yield: 53%.

**1-Ethyl-4-(3-(4-hydroxy-3-methylphenyl)pentan-3-yl)-N-neopentyl-1H-pyrrole-2-carboxamide (14b)**. By the same manner as described for the preparation of **12a**, the intermediate **14b** was prepared from the intermediate **11b**. Yield: 76%.

**N-(Cyclopropylmethyl)-1-ethyl-4-(3-(4-hydroxy-3-methylphenyl)pentan-3-yl)-1H-pyrrole-2-carboxamide (14c)**. By the same manner as described for the preparation of **12a**, the intermediate **14c** was prepared from the intermediate **11b**. Yield: 42%.

**Methyl(1-ethyl-4-(3-(4-hydroxy-3-methylphenyl)pentan-3-yl)-1H-pyrrole-2-carbonyl)glycinate (14d)**. By the same manner as described for the preparation of **12a**, the intermediate **14d** was prepared from the intermediate **11b**. Yield: 89%.

**1-Ethyl-4-(3-(4-hydroxy-3-methylphenyl)pentan-3-yl)-N-(2-hydroxyethyl)-1H-pyrrole-2-carboxamide (14d-OH)**. By the same manner as described for the preparation of **12d-OH**, the intermediate **14d-OH** was prepared from the intermediate **14d**. Yield: 87%.

**1-Ethyl-4-(3-(4-hydroxy-3-methylphenyl)pentan-3-yl)-N-(2,2,2-trifluoroethyl)-1H-pyrrole-2-carboxamide (14e)**. By the same manner as described for the preparation of **12a**, the intermediate **14e** was prepared from the intermediate **11b**. Yield: 53%.

**Methyl(1-ethyl-4-(3-(4-hydroxy-3-methylphenyl)pentan-3-yl)-1H-pyrrole-2-carbonyl)alaninate (14f)**. By the same manner as described for the preparation of **12a**, the intermediate **14f** was prepared from the intermediate **11b**. Yield: 32%.

**1-Ethyl-4-(3-(4-hydroxy-3-methylphenyl)pentan-3-yl)-N-(1-hydroxypropan-2-yl)-1H-pyrrole-2-carboxamide (14f-OH)**. By the same manner as described for the preparation of **12d-OH**, the intermediate **14f-OH** was prepared from the intermediate **14f**. Yield: 46%.

**Methyl(1-ethyl-4-(3-(4-hydroxy-3-methylphenyl)pentan-3-yl)-1H-pyrrole-2-carbonyl)valinate (14g)**. By the same manner as described for the preparation of **12a**, the intermediate **14g** was prepared from the intermediate **11b**. Yield: 49%.



1-Ethyl-N-(1-hydroxy-3-methylbutan-2-yl)-4-(3-(4-hydroxy-3-methylphenyl)pentan-3-yl)-1H-pyrrole-2-carboxamide (**14g-OH**). By the same manner as described for the preparation of **12d-OH**, the intermediate **14g-OH** was prepared from the intermediate **14g**. Yield: 61%.

1-Ethyl-4-(3-(4-hydroxy-3-methylphenyl)pentan-3-yl)-N-pentyl-1H-pyrrole-2-carboxamide (**14h**). By the same manner as described for the preparation of **12a**, the intermediate **14h** was prepared from the intermediate **11b**. Yield: 81%.

1-Ethyl-4-(3-(4-hydroxy-3-methylphenyl)pentan-3-yl)-N-(3-hydroxypropyl)-1H-pyrrole-2-carboxamide (**14i**). By the same manner as described for the preparation of **12a**, the intermediate **14i** was prepared from the intermediate **11b**. Yield: 72%.

4-(3-(4-(2,3-Dihydroxypropoxy)-3-methylphenyl)pentan-3-yl)-1-ethyl-N-(2-hydroxy-2-methylpropyl)-1H-pyrrole-2-carboxamide (**15a**). By the same manner as described for the preparation of **13a**, compound **15a** was prepared from the intermediate **14a**. Yield: 67%.

4-(3-(4-(2,3-Dihydroxypropoxy)-3-methylphenyl)pentan-3-yl)-1-ethyl-N-neopentyl-1H-pyrrole-2-carboxamide (**15b**). By the same manner as described for the preparation of **13a**, compound **15b** was prepared from the intermediate **14b**. Yield: 58%.

N-(Cyclopropylmethyl)-4-(3-(4-(2,3-dihydroxypropoxy)-3-methylphenyl)pentan-3-yl)-1-ethyl-1H-pyrrole-2-carboxamide (**15c**). By the same manner as described for the preparation of **13a**, compound **15c** was prepared from the intermediate **14c**. Yield: 47%.

4-(3-(4-(2,3-Dihydroxypropoxy)-3-methylphenyl)pentan-3-yl)-1-ethyl-N-(2-hydroxyethyl)-1H-pyrrole-2-carboxamide (**15d**). By the same manner as described for the preparation of **13a**, compound **15d** was prepared from the intermediate **14d-OH**. Yield: 54%.

4-(3-(4-(2,3-Dihydroxypropoxy)-3-methylphenyl)pentan-3-yl)-1-ethyl-N-(2,2,2-trifluoroethyl)-1H-pyrrole-2-carboxamide (**15e**). By the same manner as described for the preparation of **13a**, compound **15e** was prepared from the intermediate **14e**. Yield: 78%.

4-(3-(4-(2,3-Dihydroxypropoxy)-3-methylphenyl)pentan-3-yl)-1-ethyl-N-(1-hydroxypropan-2-yl)-1H-pyrrole-2-carboxamide (**15f**). By the same manner as described for the preparation of **13a**, compound **15f** was prepared from the intermediate **14f-OH**. Yield: 72%.

4-(3-(4-(2,3-Dihydroxypropoxy)-3-methylphenyl)pentan-3-yl)-1-ethyl-N-(1-hydroxy-3-methylbutan-2-yl)-1H-pyrrole-2-carboxamide (**15g**). By the same manner as described for the preparation of **13a**, compound **15g** was prepared from the intermediate **14g-OH**. Yield: 66%.

4-(3-(4-(2,3-Dihydroxypropoxy)-3-methylphenyl)pentan-3-yl)-1-ethyl-N-pentyl-1H-pyrrole-2-carboxamide (**15h**). By the same manner as described for the preparation of **13a**, compound **15h** was prepared from the intermediate **14h**. Yield: 76%.

4-(3-(4-(2,3-Dihydroxypropoxy)-3-methylphenyl)pentan-3-yl)-1-ethyl-N-(3-hydroxypropyl)-1H-pyrrole-2-carboxamide (**15i**). By the same manner as described for the preparation of **13a**, compound **15i** was prepared from the intermediate **14i**. Yield: 69%.

Ethyl-4-(4-(3-(1-ethyl-5-(2-hydroxy-2-methylpropyl)carbamoyl)-1H-pyrrol-3-yl)pentan-3-yl)-2-methylphenoxybutanoate (**16a**). To a solution of the intermediate **14a** (386 mg, 1 mmol) in DMF, NaH (80 mg, 2 mmol) was added portion-wise at 0 °C. The reaction mixture was stirred at 0 °C for 1 h, and then ethyl 4-bromobutyrate (291 mg, 1.5 mmol) was added. The reaction mixture was moved to 25 °C for 5 h, and then H<sub>2</sub>O (10 mL) was added. The solution was extracted with ethyl acetate, and the aqueous phase was extracted with ethyl acetate. The combined organic phases were washed with brine and then dried over anhydrous Na<sub>2</sub>SO<sub>4</sub> and evaporated. The residue was purified by column chromatography (CH<sub>2</sub>Cl<sub>2</sub>/CH<sub>3</sub>OH = 100/1) to give compound **16a** as white solid (290 mg, 58% yield).

Ethyl-5-(4-(3-(1-ethyl-5-(2-hydroxy-2-methylpropyl)carbamoyl)-1H-pyrrol-3-yl)pentan-3-yl)-2-methylphenoxy)pentanoate (**16b**). By the same manner as described for the preparation of **16a**, compound **16b** was prepared from the intermediate **14a**. Yield: 67%.

4-(4-(3-(1-Ethyl-5-(2-hydroxy-2-methylpropyl)carbamoyl)-1H-pyrrol-3-yl)pentan-3-yl)-2-methylphenoxy)butanoic Acid (**17a**). To a solution of the intermediate **16a** (200 mg, 0.4 mmol) in ethanol, KOH (67 mg, 1.2 mmol) in H<sub>2</sub>O was added, and the reaction mixture was stirred at 80 °C for 5 h. The solution was diluted with H<sub>2</sub>O (20

mL), and the pH value was adjusted to about 3–4 using 1 M HCl. Then it was extracted with ethyl acetate. The aqueous phase was extracted with ethyl acetate. The combined organic phases were washed with brine and then dried over anhydrous Na<sub>2</sub>SO<sub>4</sub> and evaporated. The residue was purified by column chromatography with petroleum ether/ethyl acetate (10/1, v/v) to give the intermediate **17a** as yellow oil (180 mg, 95%).

5-(4-(3-(1-Ethyl-5-(2-hydroxy-2-methylpropyl)carbamoyl)-1H-pyrrol-3-yl)pentan-3-yl)-2-methylphenoxy)pentanoic Acid (**17b**). By the same manner as described for the preparation of **17a**, compound **17b** was prepared from the intermediate **16b**. Yield: 87%.

4-(3-(1-Ethyl-5-(2-hydroxy-2-methylpropyl)carbamoyl)-1H-pyrrol-3-yl)pentan-3-yl)-2-methylphenyl(tert-butoxycarbonyl)alaninate (**18a**). To a solution of the intermediate **14a** (386 mg, 1 mmol) in CH<sub>2</sub>Cl<sub>2</sub> (10 mL) was added Et<sub>3</sub>N (418 μL, 3 mmol), followed by Boc-alanine (153 mg, 1.5 mmol), EDCI (288 mg, 1.5 mmol), and DMAP (12 mg, 0.1 mmol). The reaction mixture was stirred at 25 °C overnight and then poured into H<sub>2</sub>O. The solution was extracted with CH<sub>2</sub>Cl<sub>2</sub>, and aqueous phase was extracted with CH<sub>2</sub>Cl<sub>2</sub>. The combined organic phases were washed with H<sub>2</sub>O and brine and then dried over anhydrous Na<sub>2</sub>SO<sub>4</sub> and evaporated. The residue was purified by column chromatography with petroleum ether/ethyl acetate (4/1, v/v) to give compound **18a** as white solid (197 mg, 43% yield).

4-(3-(1-Ethyl-5-(2-hydroxy-2-methylpropyl)carbamoyl)-1H-pyrrol-3-yl)pentan-3-yl)-2-methylphenyl 3-((tert-butoxycarbonyl)amino)propanoate (**18b**). By the same manner as described for the preparation of **18a**, intermediate **18b** was prepared from the intermediate **14a**. Yield: 52%.

4-(3-(1-Ethyl-5-(2-hydroxy-2-methylpropyl)carbamoyl)-1H-pyrrol-3-yl)pentan-3-yl)-2-methylphenyl Alaninate (**19a**). To a solution of the intermediate **18a** (386 mg, 1 mmol) in CH<sub>2</sub>Cl<sub>2</sub> (10 mL) was added TFA (2 mL) portion-wise. The reaction mixture was stirred at 0 °C for 2 h and then poured into H<sub>2</sub>O. The solution was extracted with CH<sub>2</sub>Cl<sub>2</sub>, and aqueous phase was extracted with CH<sub>2</sub>Cl<sub>2</sub>. The combined organic phases were washed with H<sub>2</sub>O and brine and then dried over anhydrous Na<sub>2</sub>SO<sub>4</sub> and evaporated. The residue was purified by column chromatography with petroleum ether/ethyl acetate (4/1, v/v) to give compound **19a** as white solid (84 mg, 87% yield).

4-(3-(1-Ethyl-5-(2-hydroxy-2-methylpropyl)carbamoyl)-1H-pyrrol-3-yl)pentan-3-yl)-2-methylphenyl 3-aminopropanoate (**19b**). By the same manner as described for the preparation of **19a**, compound **19b** was prepared from the intermediate **18b**. Yield: 92%.

4-(4-(3-(1-Ethyl-5-(2-hydroxy-2-methylpropyl)carbamoyl)-1H-pyrrol-3-yl)pentan-3-yl)-2-methylphenoxy)-4-oxobutanoic Acid (**20**). By the same manner as described for the preparation of **16a**, compound **20** was prepared from the intermediate **14a**. Yield: 43%.

**Molecule Docking.** Molecular docking was performed with CDOCKER program, which is interfaced with Discovery Studio 3.0. The crystal structure of VDR in complex with LG190178 (ID: 2ZFX) was obtained from the Protein Data Bank (PDB). All the water and ligands were removed, and random hydrogen atoms were added. The structures of the synthesized compounds were generated and minimized using tripos force fields. The highest-scored conformation based on the CDOCKER scoring functions was selected as the final bioactive conformation.

**VDR Binding Assay.** The assay was performed using a PolarScreen VDR Competitor Assay Red kit. The assay measures the decrease in mP accompanying loss of binding to the relatively high molecular weight VDR ligand binding domain of the fluorescent tracer due to the presence of a competitor. The compounds were supplied in a 10 mM DMSO solution, and VDR binding affinity was determined by Polar Screen VDR Competitor Assay. All compounds were tested for their binding affinity at 100 nM in triplicates. The affinity observed at 100 nM was used to set relative IC<sub>50</sub> value. Fluorescence polarization was measured on an Ultra384microplate reader (Tecan) using a 535 nm excitation filter (25 nm bandwidth) and 590 nm emission filter (20 nm bandwidth). Finally, the relative IC<sub>50</sub> values of compounds were calculated using Graph Pad Prism 5.0.



**Transcription Assay.** Luciferase activity assay was performed using the Dual-Luciferase Reporter Assay System (Promega, Madison, WI) according to the manufacturer's instructions. HEK293 cells of 85–90% confluence were seeded in 48-well plates. Transfections were composed of 140 ng of TK-SPP × 3-Luciferase reporter plasmid, 20 ng of pCMX-Renilla, 30 ng of pENTER-CMV-hRXR $\alpha$ , and 100 ng of pCMX-VDR for each well using Lipofectamine2000 Reagent (Invitrogen). Eight hours after transfection, test compounds were added. Luciferase activity assay was performed 24 h later using the Dual-Luciferase Assay System. Firefly luciferase activity was normalized to the corresponding Renilla luciferase activity. All the experiments were performed three times.

**Anticollagen I Synthetic Activity Assay.** Anticollagen I synthetic activity assay was performed using the human collagen I ELISA Kit (Elabscience, Wuhan). LX-2 cells obtained from American Type Culture Collection were maintained in Gibco 1640 medium supplement with 10% fetal bovine serum (FBS) and 1% penicillin–streptomycin. Approximately  $1 \times 10^5$  cells, suspended in medium were plated into each well of a 24-well plate and grown at 37 °C in humidified atmosphere with 5% CO<sub>2</sub> for 24 h. The following day, tested compounds at the concentration of 100 nM were added to the culture medium and incubated for 24 h. Supernate was centrifuged for 20 min to remove insoluble impurity and cell debris at 1000g at 2–8 °C. The clear supernate was suspended and the assay was immediately carried out following the description of the Kit. Finally, the optical density (OD) was measured spectrophotometrically at a wavelength of  $450 \pm 2$  nm. The OD value is proportional to the concentration of human collagen I.

**Small Interfering RNA (siRNA) Transfection.** A VDR-directed siRNA and a scrambled siRNA were purchased from RIBOBIO Biotechnologies (Guangzhou, China). Transfection was carried out at a concentration of 50 nM using Lipofectamine2000 Reagent (Invitrogen). Transfected cells were cultured 24 h prior to terminal assays.

**CCl<sub>4</sub>-Induced Mouse Hepatic Fibrosis Model.** This study was carried out in strict accordance with the recommendations in the Guide for the Care and Use of Laboratory Animals of the National Institutes of Health. The protocol was approved by the Experimentation Ethics Review Committee of China Pharmaceutical University. All surgery was performed under sodium pentobarbital anesthesia, and all efforts were made to minimize suffering.

Male C57BL/6J mice (8 weeks old) were purchased from the Medical School of Yangzhou University (Yangzhou, China). All mice were maintained under standard conditions with free access to water and laboratory rodent food. To set up CCl<sub>4</sub>-induced mouse hepatic fibrosis model, mice were IP injected with 0.5 mL/kg bodyweight CCl<sub>4</sub> (1:50 v/v in corn oil from Sigma) three times a week for 4 weeks. Control mice received vehicle (DMSO in corn oil) instead. The effect of vitamin D analogues on CCl<sub>4</sub>-induced mouse hepatic fibrosis was evaluated 20 days after the first dose of CCl<sub>4</sub>, calcipotriol, 1,25(OH)<sub>2</sub>D<sub>3</sub>, or compound 15a (20  $\mu$ g/kg body weight) was administered by oral gavage five times a week. Mice were sacrificed 72 h after the final CCl<sub>4</sub> injection. Mouse livers and serum were obtained for histopathology, collagen assay, biochemical, and molecular analyses.

**Lab Data Detection of Serum Sample.** Serum was collected from blood after centrifugation at 3000 rpm for 15 min at 4 °C. Serum alanine amino transferase (ALT), aspartic transaminase (AST), and total bile acid (TBA) were detected using commercial kits according to the manufacturer's instructions.

**Histology.** Livers were fixed in 4% (w/v) neutral phosphate-buffered paraformaldehyde for 24 h, dehydrated, transparentized, and embedded in paraffin. Liver tissues were cut into 5  $\mu$ m sections, which were stained with hematoxylin-eosin (H&E) for structured observation, or with Masson's trichrome stain for detection of collagen deposits. Determination of hydroxyproline content was carried out using a kit from Nanjing Jian Cheng Bioengineering Institute (Nanjing, China) according to the instruction by the manufacturer.

**Immunohistochemistry Analysis.** Immunohistochemistry staining for detection of HSC activation *in vivo* was performed as

previously described. Briefly, paraffin was removed from the slides, subjected to antigen retrieval, and quenched of endogenous peroxidase activity using 3% (v/v) H<sub>2</sub>O<sub>2</sub> for 10 min. Immune complexes were visualized using suitable peroxidase-coupled secondary antibodies, according to the manufacturer's protocol (SP-9000 D 2-step plus poly-HR Panti-mouse/rabbit IgG detection system, ZSGB-BIO; Beijing, China). Mouse anti- $\alpha$ -SMA was employed as the primary antibody (Boster, Wuhan, China). The secondary antibodies incubated were horseradish peroxidase-conjugated goat antimouse IgG (Boster, Wuhan, China).

**RNA Extraction and Quantitative Real-Time Polymerase Chain Reaction (Q-PCR).** cDNA was generated from RNA extracts derived from cultured LX-2 cells and liver tissues using a reverse transcription kit (Transgen, Beijing, China).  $\beta$ -actin (mouse) or U36B4 (human) was used as an internal control. Q-PCR was performed using the SYBR Green Master Mix (Vazyme). Primer pairs of mRNA used are as shown in Table S2.

**Western Blot.** Proteins were purified from LX-2 cells. Proteins were separated using 10% SDS-polyacrylamide gel electrophoresis and were electrophoretically transferred to polyvinylidene fluoride (PVDF) membranes using standard procedures. The following primary antibodies were employed: mouse anti- $\alpha$ -SMA (Boster, Wuhan, China), rabbit anti-collagen I (Boster, Wuhan, China), mouse anti-VDR (Santa Cruz, Inc.), and mouse anti- $\beta$ -actin (Boster, Wuhan, China). Horseradish peroxidase-conjugated goat antirabbit/mouse IgG (Boster, Wuhan, China) was used as the secondary antibody. Immunoreactive protein bands were detected using an Odyssey Scanning System (LI-COR Inc.).

**Pharmacokinetics Study.** Compound 15a and 1,25(OH)<sub>2</sub>D<sub>3</sub> were dissolved in ethanol/EL/saline (1:1:18). Male Sprague–Dawley (SD) rats ( $n = 3$ ) weighing 180–220 g were injected with these compounds intravenously (5 mg/kg) or intragastrically (20 mg/kg). Blood plasma samples were collected at 5, 15, and 30 min and 1 h, 2 h, 4 h, 8 h, 12 h, and 24 h after administration of compounds and then immediately centrifuged (12000 rpm, 10 min) to obtain plasma samples. The concentration of compounds in plasma was measured by HPLC. The pharmacokinetic parameters were calculated using Kinetic 4.4 software.

**Statistical Analysis.** Data were expressed as means  $\pm$  SD from at least three independent experiments. The differences between groups were analyzed for significance by *t* test when only two groups were compared or by one-way analysis of variance (ANOVA). All statistical analysis was performed using SPSS for Windows version 11.0 (SPSS, Chicago, IL).

## ■ ASSOCIATED CONTENT

### 📄 Supporting Information

The Supporting Information is available free of charge on the ACS Publications website at DOI: 10.1021/acs.jmedchem.8b01165.

Cytotoxicities of synthesized compounds against LX-2 cells. Primers used for PCR analysis. Pharmacokinetic parameters of compounds 15a and 1,25(OH)<sub>2</sub>D<sub>3</sub> in rats. Relative expression of *CYP24A1* mRNA in LX-2 cells incubated with compound for 24 h measured by Q-PCR. Relative expression of *Cyp24a1* mRNA in liver measured by Q-PCR. Relative expression of *Trpv6* mRNA in mouse intestine measured by Q-PCR. H NMR and <sup>13</sup>C NMR spectra of compounds (PDF)

Molecular formula strings (CSV)

Compound 15a (PDB)

## ■ AUTHOR INFORMATION

### Corresponding Author

\*Tel/Fax: 86-25-83271171. E-mail: zhangcan@cpu.edu.cn.

ORCID 

Can Zhang: 0000-0003-3529-5438

## Author Contributions

<sup>§</sup>These authors contributed equally to this work. The manuscript was written through contributions of all authors. All authors have given approval to the final version of the manuscript.

## Notes

The authors declare no competing financial interest.

## ACKNOWLEDGMENTS

The authors thank Public platform of State Key Laboratory of Natural Medicine. This work was supported by the National Natural Science Foundation of China (81273468, 81473153, 81703585), National Basic Research Program of China (2015CB755500), Fundamental Research Funds for the Central Universities of China (2632017PY10), 111 Project from the Ministry of Education of China and the State Administration of Foreign Expert Affairs of China (No. 111-2-07), the fund of Fujian Provincial Key Laboratory of Hepatic Drug Research (KFLX2018002), and the Open Project of State Key Laboratory of Natural Medicines (No. SKLNMZZCX201811).

## ABBREVIATIONS USED

ALT, alanine transaminase; AST, aspartate transaminase; CCl<sub>4</sub>, carbon tetrachloride; DRIPs, VDR interacting proteins; ECM, extracellular matrix; HSCs, hepatic stellate cells; IP, intra-peritoneal; LBP, ligand binding pocket; NAFLD, nonalcoholic fatty liver disease; NASH, nonalcoholic steatohepatitis; RNAi, RNA interference; SARs, structure-activity relationships; TBA, total bile acid; TGF, transforming growth factor; VDR, vitamin D receptor

## REFERENCES

- (1) Bataller, R.; Brenner, D. A. Liver fibrosis. *J. Clin. Invest.* **2005**, *115*, 209–218.
- (2) Hernandez-Gea, V.; Friedman, S. L. Pathogenesis of liver fibrosis. *Annu. Rev. Pathol. Mech. Dis.* **2011**, *6*, 425–456.
- (3) Lee, U. E.; Friedman, S. L. Mechanisms of hepatic fibrogenesis. *Best practice & research Clinical gastroenterology* **2011**, *25*, 195–206.
- (4) Friedman, S. L. Liver fibrosis – from bench to bedside. *J. Hepatol.* **2003**, *38* (Suppl 1), S38–53.
- (5) Siegmund, S. V.; Dooley, S.; Brenner, D. A. Molecular mechanisms of alcohol-induced hepatic fibrosis. *Digestive diseases* **2006**, *23*, 264–274.
- (6) Friedman, S. L.; Bansal, M. B. Reversal of hepatic fibrosis – fact or fantasy? *Hepatology* **2006**, *43*, S82–88.
- (7) Said, A.; Lucey, M. R. Liver transplantation: an update 2008. *Curr. Opin. Gastroenterol.* **2008**, *24*, 339–345.
- (8) Williams, R. Global challenges in liver disease. *Hepatology* **2006**, *44*, 521–526.
- (9) Cohen-Naftaly, M.; Friedman, S. L. Current status of novel antifibrotic therapies in patients with chronic liver disease. *Ther. Adv. Gastroenterol.* **2011**, *4*, 391–417.
- (10) Friedman, S. L. Hepatic stellate cells: protean, multifunctional, and enigmatic cells of the liver. *Physiol. Rev.* **2008**, *88*, 125–172.
- (11) Zhang, D. Y.; Friedman, S. L. Fibrosis-dependent mechanisms of hepatocarcinogenesis. *Hepatology* **2012**, *56*, 769–775.
- (12) Breitkopf, K.; Godoy, P.; Ciuclan, L.; Singer, M. V.; Dooley, S. TGF-beta/smud signaling in the injured liver. *Z. Gastroenterol.* **2006**, *44*, 57–66.
- (13) Inagaki, Y.; Okazaki, I. Emerging insights into transforming growth factor beta smad signal in hepatic fibrogenesis. *Gut* **2007**, *56*, 284–292.

- (14) Cao, H.; Yu, J.; Xu, W.; Jia, X.; Yang, J.; Pan, Q.; Zhang, Q.; Sheng, G.; Li, J.; Pan, X.; Wang, Y.; Li, L. Proteomic analysis of regenerating mouse liver following 50% partial hepatectomy. *Proteome Sci.* **2009**, *7*, 48.

- (15) Abramovitch, S.; Dahan-Bachar, L.; Sharvit, E.; Weisman, Y.; Ben Tov, A.; Brazowski, E.; Reif, S. Vitamin D inhibits proliferation and profibrotic marker expression in hepatic stellate cells and decreases thioacetamide-induced liver fibrosis in rats. *Gut* **2011**, *60*, 1728–1737.

- (16) Halder, S. K.; Goodwin, J. S.; Al-Hendy, A. 1,25-Dihydroxyvitamin D3 reduces TGF-beta3-induced fibrosis-related gene expression in human uterine leiomyoma cells. *J. Clin. Endocrinol. Metab.* **2011**, *96*, E754–762.

- (17) Byers, T. Anticancer vitamins du Jour–The ABCED’s so far. *Am. J. Epidemiol.* **2010**, *172*, 1–3.

- (18) Feldman, D.; Krishnan, A. V.; Swami, S.; Giovannucci, E.; Feldman, B. J. The role of vitamin D in reducing cancer risk and progression. *Nat. Rev. Cancer* **2014**, *14*, 342–357.

- (19) Gascon-Barre, M.; Demers, C.; Mirshahi, A.; Neron, S.; Zalzal, S.; Nanci, A. The normal liver harbors the vitamin D nuclear receptor in nonparenchymal and biliary epithelial cells. *Hepatology* **2003**, *37*, 1034–1042.

- (20) Ding, N.; Yu, R. T.; Subramaniam, N.; Sherman, M. H.; Wilson, C.; Rao, R.; Leblanc, M.; Coulter, S.; He, M.; Scott, C.; Lau, S. L.; Atkins, A. R.; Barish, G. D.; Gunton, J. E.; Liddle, C.; Downes, M.; Evans, R. M. A vitamin D receptor/smud genomic circuit gates hepatic fibrotic response. *Cell* **2013**, *153*, 601–613.

- (21) Perakyla, M.; Malinen, M.; Herzig, K. H.; Carlberg, C. Gene regulatory potential of nonsteroidal vitamin D receptor ligands. *Mol. Endocrinol.* **2005**, *19*, 2060–2073.

- (22) Sato, M.; Lu, J.; Iturria, S.; Stayrook, K. R.; Burris, L. L.; Zeng, Q. Q.; Schmidt, A.; Barr, R. J.; Montrose-Rafizadeh, C.; Bryant, H. U.; Ma, Y. L. A nonsecosteroidal vitamin D receptor ligand with improved therapeutic window of bone efficacy over hypercalcemia. *J. Bone Miner. Res.* **2010**, *25*, 1326–1336.

- (23) Na, S.; Ma, Y.; Zhao, J.; Schmidt, C.; Zeng, Q. Q.; Chandrasekhar, S.; Chin, W. W.; Nagpal, S. A nonsecosteroidal vitamin d receptor modulator ameliorates experimental autoimmune encephalomyelitis without causing hypercalcemia. *Autoimmune Dis.* **2011**, *2011*, 132958.

- (24) Plum, L. A.; DeLuca, H. F. Vitamin D, disease and therapeutic opportunities. *Nat. Rev. Drug Discovery* **2010**, *9*, 941–955.

- (25) Carlberg, C.; Molnar, F. Current status of vitamin D signaling and its therapeutic applications. *Curr. Top. Med. Chem.* **2012**, *12*, 528–547.

- (26) Belorusova, A. Y.; Rochel, N. Modulators of vitamin D nuclear receptor: recent advances from structural studies. *Curr. Top. Med. Chem.* **2014**, *14*, 2368–2377.

- (27) Yamada, S.; Makishima, M. Structure-activity relationship of nonsecosteroidal vitamin D receptor modulators. *Trends Pharmacol. Sci.* **2014**, *35*, 324–337.

- (28) Makishima, M. Current Topics on Vitamin D. Nonsecosteroidal vitamin D modulators and prospects for their therapeutic application. *Clinical calcium* **2015**, *25*, 403–411.

- (29) Boehm, M. F.; Fitzgerald, P.; Zou, A.; Elgort, M. G.; Bischoff, E. D.; Mere, L.; Mais, D. E.; Bissonnette, R. P.; Heyman, R. A.; Nadzan, A. M.; Reichman, M.; Allegretto, E. A. Novel nonsecosteroidal vitamin D mimics exert VDR-modulating activities with less calcium mobilization than 1,25-dihydroxyvitamin D3. *Chem. Biol.* **1999**, *6*, 265–275.

- (30) Fujii, S.; Masuno, H.; Taoda, Y.; Kano, A.; Wongmayura, A.; Nakabayashi, M.; Ito, N.; Shimizu, M.; Kawachi, E.; Hirano, T.; Endo, Y.; Tanatani, A.; Kagechika, H. Boron cluster-based development of potent nonsecosteroidal vitamin D receptor ligands: direct observation of hydrophobic interaction between protein surface and carborane. *J. Am. Chem. Soc.* **2011**, *133*, 20933–20941.

- (31) Fujii, S.; Kano, A.; Masuno, H.; Songkram, C.; Kawachi, E.; Hirano, T.; Tanatani, A.; Kagechika, H. Design and synthesis of tetraol derivatives of 1,12-dicarba-closo-dodecaborane as non-

secosteroidal vitamin D analogs. *Bioorg. Med. Chem. Lett.* **2014**, *24*, 4515–4519.

(32) Fujii, S.; Kano, A.; Songkram, C.; Masuno, H.; Taoda, Y.; Kawachi, E.; Hirano, T.; Tanatani, A.; Kagechika, H. Synthesis and structure-activity relationship of p-carborane-based non-secosteroidal vitamin D analogs. *Bioorg. Med. Chem.* **2014**, *22*, 1227–1235.

(33) Fujii, S.; Sekine, R.; Kano, A.; Masuno, H.; Songkram, C.; Kawachi, E.; Hirano, T.; Tanatani, A.; Kagechika, H. Structural development of p-carborane-based potent non-secosteroidal vitamin D analogs. *Bioorg. Med. Chem.* **2014**, *22*, 5891–5901.

(34) Shen, W.; Xue, J.; Zhao, Z.; Zhang, C. Novel nonsecosteroidal VDR agonists with phenyl-pyrrolyl pentane skeleton. *Eur. J. Med. Chem.* **2013**, *69*, 768–778.

(35) Ge, Z.; Hao, M.; Xu, M.; Su, Z.; Kang, Z.; Xue, L.; Zhang, C. Novel nonsecosteroidal VDR ligands with phenyl-pyrrolyl pentane skeleton for cancer therapy. *Eur. J. Med. Chem.* **2016**, *107*, 48–62.

(36) Hao, M.; Hou, S.; Xue, L.; Yuan, H.; Zhu, L.; Wang, C.; Wang, B.; Tang, C.; Zhang, C. Further developments of the phenyl-pyrrolyl pentane series of nonsteroidal vitamin d receptor modulators as anticancer agents. *J. Med. Chem.* **2018**, *61*, 3059–3075.

(37) Kudo, T.; Ishizawa, M.; Maekawa, K.; Nakabayashi, M.; Watarai, Y.; Uchida, H.; Tokiwa, H.; Ikura, T.; Ito, N.; Makishima, M.; Yamada, S. Combination of triple bond and adamantane ring on the vitamin D side chain produced partial agonists for vitamin D receptor. *J. Med. Chem.* **2014**, *57*, 4073–4087.

(38) Liu, C.; Zhao, G. D.; Mao, X.; Suenaga, T.; Fujishima, T.; Zhang, C. M.; Liu, Z. P. Synthesis and biological evaluation of 1 $\alpha$ ,25-dihydroxyvitamin D<sub>3</sub> analogues with aromatic side chains attached at C-17. *Eur. J. Med. Chem.* **2014**, *85*, 569–575.

(39) Watarai, Y.; Ishizawa, M.; Ikura, T.; Zacconi, F. C.; Uno, S.; Ito, N.; Mourino, A.; Tokiwa, H.; Makishima, M.; Yamada, S. Synthesis, biological activities, and x-ray crystal structural analysis of 25-hydroxy-25(or 26)-adamantyl-17-[20(22),23-diyanyl]-21-norvitamin D compounds. *J. Med. Chem.* **2015**, *58*, 9510–9521.

(40) Salem, N. A.; Hamza, A.; Alnahdi, H.; Ayaz, N. Biochemical and molecular mechanisms of platelet-rich plasma in ameliorating liver fibrosis induced by dimethylnitrosurea. *Cell. Physiol. Biochem.* **2018**, *47*, 2331–2339.

(41) Ma, Y.; Khalifa, B.; Yee, Y. K.; Lu, J.; Memezawa, A.; Savkur, R. S.; Yamamoto, Y.; Chintalacharuvu, S. R.; Yamaoka, K.; Stayrook, K. R.; Bramlett, K. S.; Zeng, Q. Q.; Chandrasekhar, S.; Yu, X. P.; Linebarger, J. H.; Iturria, S. J.; Burris, T. P.; Kato, S.; Chin, W. W.; Nagpal, S. Identification and characterization of noncalcemic, tissue-selective, nonsecosteroidal vitamin D receptor modulators. *J. Clin. Invest.* **2006**, *116*, 892–904.